Graphical Techniques for the Assessment of Bayesian Optimal Designs

by

Nasiba Maruf Ahmed

Submitted in fulfilment of the MSc. degree in Statistics

Department of Statistics
University of Manitoba
Winnipeg

Abstract

Response surface methodology is a well-developed paradigm of statistical design and analysis that involves design of experiments, collection of data, conduction of regression analysis and evaluation of the fitted relationship between the factors and the response. Prediction capability is considered a vital aspect in response surface methodology as it reveals essential aspects of a process or system. Comparisons of designs' prediction efficiency based on single-valued efficiency-type criteria may not be always desirable. Thus, graphical techniques like variance dispersion graphs and fraction of design space plots were introduced which focus on the evaluation of the prediction performance of the designs. These graphical tools display the prediction capability of the designs over the entire design region.

Popular optimal designs, such as D-optimal designs, are constructed based on an assumed model. To reduce the model dependency, Bayesian designs were proposed. However, the variance dispersion graphs and the fraction of design space plots in the literature are not applicable to Bayesian designs. In this thesis, we developed the graphs for Bayesian designs. We created the graphs for 24-run 3-level Bayesian optimal designs with 3 factors and 30-run 3-level Bayesian optimal designs with 4 factors. Comparisons are made among the Bayesian optimal designs.

Acknowledgment

I would like to begin by expressing my wholehearted gratitude to my research supervisor Dr. Po Yang. I went through a very crucial stage of my personal life while my research endeavor began, when I gave birth to a baby boy in 2020. Continuing the research with a newborn, that too in pandemic was becoming hectic for me. Her untethered support helped me remain sane and overcome the turbulant phase of my life. I will be forever grateful for her immense understanding and patience.

I would like to thank Dr. Saumen Mandal and Dr. Max Turgeon for serving in my thesis examining committee and taking the time to provide valuable feedback on my thesis.

I am thankful to the Department of Statistics for the financial support, administrative assistant Ms. Margaret Smith and graduate assistant Ms. Rosa Di Noto for their support.

Last but not the least, I would like to thank my family, specially my husband Nazmush Sakib Joy, who always stood by me as my best friend, my guide and my support system.

Finally, my thanks also goes to all my friends and all the people who have willingly helped me with their abilities directly or indirectly.

Contents

List of Tables

List of Figures

Chapter 1

Introduction

Application of a well organized and planned experimental design is crucial for the proper implementation of any scientific method. Hypothesizing the methodology for what has been observed is a part of the scientific method, where a statistical experimental design ensures the collection of the data in a manner that addresses the hypothesis in question through statistical analysis. Thereby, analysis of experiment presents the basis of valid inference and prediction in various fields like medicine, engineering, business, and agriculture.

Acquiring an optimal experimental design is a vital aspect in the area of experimental design. Optimal design is the design that attains some targets of interest. The concept of optimality in experimental designs was first introduced by Smith (1918), who considered selecting experimental designs that minimize the maximum prediction variance over the design space. This criterion was later named by Kiefer and Wolfowitz (1959) as global or G-optimality. Several criteria have been proposed for evaluation and selection of

optimal design. One category is focused on the minimization of the variance of the parameter estimates and the other category is based on the prediction properties of the design. Wald (1943) was the first to introduce one of the criteria from the former category, popularly known as D-optimality criterion which minimizes the variance of the parameter estimates. On the other hand, I-optimality criterion, that indicates the integrated variance, belong to the latter category that prioritizes the minimization of the average prediction variance of the response. Owing to the significance of prediction of response in scientific research, this criterion has gained popularity in recent times. Jones and Goos (2012) showed that I-optimal split-plot designs perform better than D-optimal split-plot designs in terms of enhanced prediction along with precision of factor effect estimates. A modified optimality criterion named as I_D-optimality criterion proposed by Trinca and Gilmour (1999) focuses on the minimization of the average prediction variance of the difference of responses.

Replicated experiments are crucial for the estimation of experimental error. But, full replicated designs are often costlier and time consuming. In such situations, partially replicated designs offer an alternative for the estimation of error variance based on pure replicates at reduced cost and time. Lupinacci and Pigeon (2008) proposed partially replicated designs based on hadamard matrices that yields an $n/4$ replicate. A compound criterion named extended minimum aberration was introduced by Tsai and Liao (2014) for selecting partially replicated designs. In order to obtain replicated designs,

Gilmour and Trinca (2012) adjusted the D-optimality criterion and introduced DP-optimality criterion. Adopting similar idea, de Oliveira et al. (2019) proposed IP-optimality criterion which helps to obtain more replicated points.

In order to eradicate the issue of dependency on model assumption in the classical method, DuMouchel and Jones (1994) introduced a modified Bayesian D-criterion by splitting the terms in the model into primary and potential terms. Bayesian approach is explicitly applicable when the researcher has some prior information and useful when the focus is on predictive purposes, especially in situations like clinical trials and sequential experimentation (Chaloner and Verdinelli, 1995). This approach can efficiently accommodate data from previous experiments and also take an account of ethical considerations. Leonard and Edwards (2017) incorporated the idea of Gilmour and Trinca (2012) and proposed the Bayesian DP-optimality criterion by modifying the Bayesian D-optimality criterion, for acquiring partially replicated designs. Employing this concept, Basnayake (2019) modified Bayesian I-optimality criterion and proposed Bayesian IP-, I_D-, and I_DP-optimality criteria.

I-optimality criterion aims to select designs with high prediction efficiency. However, the selected optimal designs may not always serve the purpose, since researchers may not know in advance where in the design space predictions will need to be made. Moreover, multiple optimal designs may be obtained from one optimality criterion. Subsequently, grapical techniques like variance

dispersion graph (Giovannitti-Jensen and Myers, 1989) and fraction of design space plot (Zahran et al., 2003) were introduced for the evaluation of the experimental designs over the whole design region. These techniques analyze scaled prediction variance (SPV) of the response. Some statistical software, such as R, can produce such graphs. However, these graphical tools are not applicable for the assessment of Bayesian experimental designs.

Implementing the idea of variance dispersion graph, quantile plots and fraction of design space plot into Bayesian concept, we proposed the graphical techniques for the appraisal of Bayesian experimental designs in this thesis. These graphical techniques will facilitate the depiction of prediction capacity of a Bayesian design over the whole region of interest.

After quantifying the ranges of the factors that lead to the optimum outcome through first order modelling, second order models are employed to comprehend the curvature present in the response variables. Accurate predictions are crucial for locating the optimum of the response surface. Hence, prediction variance is paramount for the second order models rather than the first order models. We primarily focused on 24-run 3-level Bayesian optimal designs with 3 factors and 30-run 3-level Bayesian optimal designs with 4 factors obtained by Basnayake (2019). We obtained the variance dispersion graph and fraction of design space plot for the assessment of Bayesian optimal designs. The comparisons of the designs on the prediction capability over the whole design space are made.

The thesis is organized as follows. Chapter 2 includes an exhaustive elaboration on the optimality criteria used in classical and Bayesian approaches. This chapter also highlights the graphical techniques used for the assessment of optimal designs. Chapter 3 introduces the graphical techniques for the evaluation of Bayesian optimal designs. The graphs of the 3-level Bayesian I-, Bayesian D-, Bayesian IP-, Bayesian DP-, Bayesian I_D- and Bayesian I_DP-optimal designs in Basnayake (2019) are constructed. In Chapter 4, we compare the Bayesian D-, IP-, DP-, I_D- and I_DP-optimal designs with Bayesian I-optimal design using the variance dispersion graph, fraction of design space plot and quantile plot. Chapter 5 contains the comparison of the Bayesian optimal designs with I-optimal design. Finally, we make our concluding remarks and suggest possible future work in Chapter 6.

Chapter 2

Optimality Criteria and Graphical Assessment Techniques

In this chapter, we will introduce optimality criteria and some graphical tools such as variance dispersion graph and fraction of design space plot. Section 2.1 contains a brief overview of D-, DP-, I-, IP-, I_D- and I_DP-optimality criteria. Section 2.2 introduces Bayesian D-, Bayesian DP-, Bayesian I-, Bayesian IP-, Bayesian I_D- and Bayesian I_DP-optimality criteria. Graphical techniques for the assessment of experimental designs are presented in section 2.3.

2.1 Optimality Criteria

D-Optimality Criterion

The D-optimality criterion was introducted by Wald (1943) while comparing designs using the determinant of the information matrix. Consider the model

$$\boldsymbol{Y} = \boldsymbol{X}\boldsymbol{\beta} + \boldsymbol{\epsilon},$$

where $\boldsymbol{Y}$ is an $n \times 1$ response vector, $\boldsymbol{X}$ is the $n \times p$ model matrix, n and p are the number of experimental runs and the number of unknown model parameters, respectively, $\boldsymbol{\beta}$ is the $p \times 1$ vector of unknown model parameters and $\boldsymbol{\epsilon} \sim N(\mathbf{0}, \sigma^2\boldsymbol{I})$ is the random error vector.

The D-optimality criterion attempts to minimize the variance of the parameter estimates. It is known that the least square estimate of $\boldsymbol{\beta}$ is

$$\hat{\boldsymbol{\beta}} = (\boldsymbol{X}'\boldsymbol{X})^{-1}\boldsymbol{X}'\boldsymbol{Y}$$

and the variance-covariance matrix of $\hat{\boldsymbol{\beta}}$ is

$$Var(\hat{\boldsymbol{\beta}}) = \sigma^2(\boldsymbol{X}'\boldsymbol{X})^{-1}.$$

Thus D-optimal design maximizes the information matrix $|\boldsymbol{X}'\boldsymbol{X}|$, which is equivalent to minimizing the variance of the parameter estimates.

DP-Optimality Criterion

Partially replicated designs provide a pathway for the estimation of error variance based on pure replicates at reduced cost and time in comparison to fully replicated designs. Gilmour and Trinca (2012) defined the DP-optimality criterion which attempts to minimize the volume of the confidence region in order to attain partially replicated designs or more replicated points. The DP-optimality criterion maximizes

$$\frac{|\boldsymbol{X}'\boldsymbol{X}|}{(F_{p,d;1-\alpha})^p},$$

where d is the pure error degrees of freedom and $F_{p,d;1-\alpha}$ is the $(1-\alpha)$ quantile of F-distribution.

I-Optimality Criterion

The I-optimality criterion is a response based criterion that focuses on reducing prediction variance. It minimizes the average variance of prediction over the entire experimental region.

Let $\boldsymbol{f}(\boldsymbol{x})$ be the basis expansion of the vector $\boldsymbol{x}$ in the design region χ to the corresponding model vector. Then the predicted response $\hat{y}(\boldsymbol{x}) = \boldsymbol{f}'(\boldsymbol{x})\hat{\boldsymbol{\beta}}$.

Thus, the variance of the predicted response $\hat{y}(\boldsymbol{x})$ can be written as

$$\begin{aligned} Var(\hat{y}(\boldsymbol{x})) &= Var(\boldsymbol{f}'(\boldsymbol{x})\hat{\boldsymbol{\beta}}) \\ &= \boldsymbol{f}'(\boldsymbol{x})Var(\hat{\boldsymbol{\beta}})\boldsymbol{f}(\boldsymbol{x}) \\ &= \sigma^2\boldsymbol{f}'(\boldsymbol{x})(\boldsymbol{X}'\boldsymbol{X})^{-1}\boldsymbol{f}(\boldsymbol{x}). \end{aligned} \tag{2.1}$$

The average variance of prediction (Jones and Goos, 2012) is

$$\begin{aligned} \text{Average Prediction Variance} &= \frac{\int_{\boldsymbol{x}\epsilon\chi} Var(\hat{y}(\boldsymbol{x}))d\boldsymbol{x}}{\int_{\boldsymbol{x}\epsilon\chi} d\boldsymbol{x}} \\ &= \frac{\int_{\boldsymbol{x}\epsilon\chi} \sigma^2\boldsymbol{f}'(\boldsymbol{x})(\boldsymbol{X}'\boldsymbol{X})^{-1}\boldsymbol{f}(\boldsymbol{x})d\boldsymbol{x}}{\int_{\boldsymbol{x}\epsilon\chi} d\boldsymbol{x}}, \end{aligned} \tag{2.2}$$

where $\int_{\boldsymbol{x}\epsilon\chi} d\boldsymbol{x}$ is the volume of the design region χ.

As $\boldsymbol{f}'(\boldsymbol{x})(\boldsymbol{X}'\boldsymbol{X})^{-1}\boldsymbol{f}(\boldsymbol{x})$ is a scaler, we can write

$$\boldsymbol{f}'(\boldsymbol{x})(\boldsymbol{X}'\boldsymbol{X})^{-1}\boldsymbol{f}(\boldsymbol{x}) = tr(\boldsymbol{f}'(\boldsymbol{x})(\boldsymbol{X}'\boldsymbol{X})^{-1}\boldsymbol{f}(\boldsymbol{x}).$$

By cyclically permuting matrices, we obtain

$$tr(\boldsymbol{f}'(\boldsymbol{x})(\boldsymbol{X}'\boldsymbol{X})^{-1}\boldsymbol{f}(\boldsymbol{x})) = tr((\boldsymbol{X}'\boldsymbol{X})^{-1}\boldsymbol{f}(\boldsymbol{x})\boldsymbol{f}'(\boldsymbol{x})).$$

It follows that

$$\begin{aligned}\int_{\boldsymbol{x}\epsilon\chi} \boldsymbol{f}'(\boldsymbol{x})(\boldsymbol{X}'\boldsymbol{X})^{-1}\boldsymbol{f}(\boldsymbol{x})d\boldsymbol{x} &= \int_{\boldsymbol{x}\epsilon\chi} tr[(\boldsymbol{X}'\boldsymbol{X})^{-1}\boldsymbol{f}(\boldsymbol{x})\boldsymbol{f}'(\boldsymbol{x})]d\boldsymbol{x} \\ &= tr[\int_{x\epsilon\chi} (\boldsymbol{X}'\boldsymbol{X})^{-1}\boldsymbol{f}(\boldsymbol{x})\boldsymbol{f}'(\boldsymbol{x})d\boldsymbol{x}] \\ &= tr[(\boldsymbol{X}'\boldsymbol{X})^{-1}\int_{\boldsymbol{x}\epsilon\chi} \boldsymbol{f}(\boldsymbol{x})\boldsymbol{f}'(\boldsymbol{x})d\boldsymbol{x}].\end{aligned}$$

Thus, the average prediction variance is proportional to $tr[(\boldsymbol{X}'\boldsymbol{X})^{-1}\boldsymbol{B}]$,

where

$$\boldsymbol{B} = \frac{\int_{\boldsymbol{x}\epsilon\chi} \boldsymbol{f}(\boldsymbol{x})\boldsymbol{f}'(\boldsymbol{x})d\boldsymbol{x}}{\int_{\boldsymbol{x}\epsilon\chi} d\boldsymbol{x}} \tag{2.3}$$

is a $p \times p$ matrix of region moments. When the design space is $[-1, 1]^m$, m being the number of factors, and a full quadratic model is considered,

$$\boldsymbol{B} = \begin{bmatrix} \mathbf{1} & \mathbf{0}'_m & \mathbf{0}'_{m^*} & (1/3)\mathbf{1}'_m \\ \mathbf{0}_m & (1/3)\boldsymbol{I}_m & \mathbf{0}_{m\times m^*} & \mathbf{0}_{m\times m} \\ \mathbf{0}_{m^*} & \mathbf{0}_{m^*\times m} & (1/9)\boldsymbol{I}_{m^*} & \mathbf{0}_{m^*\times m} \\ (1/3)\mathbf{1}_m & \mathbf{0}_{m\times m} & \mathbf{0}_{m\times m^*} & (1/45)(4\boldsymbol{I}_m + 5\boldsymbol{J}_m), \end{bmatrix},$$

where m^* is the number of two-factor interactions and J is an $m \times m$ matrix of ones. I-optimal design is defined to minimize

$$tr[(\boldsymbol{X}'\boldsymbol{X})^{-1}\boldsymbol{B}].$$

Table 2.1: A 24-run I-optimal design with 3 factors

Run	X1	X2	X3
1	0	1	1
2	-1	-1	0
3	1	0	0
4	1	-1	1
5	1	1	-1
6	0	-1	1
7	-1	0	-1
8	-1	0	-1
9	-1	1	0
10	0	0	0
11	0	0	0
12	1	0	1
13	-1	1	1
14	0	0	0
15	0	1	-1
16	1	1	0
17	0	-1	0
18	-1	-1	0
19	0	0	0
20	1	-1	-1
21	0	-1	-1
22	0	0	-1
23	-1	0	1
24	0	0	0

IP-Optimality Criterion

Gilmour and Trinca (2012) and de Oliveira et al. (2019) considered the performance of a design for interval predictions. They modified the I-criterion and defined the IP-criterion which minimize the average of the width of pointwise confidence intervals for the mean response over whole design region, that is, minimize

$$tr[(\boldsymbol{X}'\boldsymbol{X})^{-1}\boldsymbol{B}]F_{1,d;1-\alpha}.$$

The IP-criterion can also help to select more replicated points when searching for optimal designs.

I_D-Optimality Criterion

Trinca and Gilmour (1999) suggested that differences between the estimated response at standard condition and at other non-standard conditions can reveal significant insights. Utilizing this idea, they defined the I_D-optimality criterion that minimizes the average difference variance in response. Let the difference between the estimated response at standard operating condition of the process $\boldsymbol{x}_0$ and the estimated response at any other location $\boldsymbol{x}$ be $y(\boldsymbol{x}) - y(\boldsymbol{x}_0)$. Then the average difference variance is

$$\frac{\int_{\boldsymbol{x}\epsilon\chi} Var(\hat{y}(\boldsymbol{x}) - \hat{y}(\boldsymbol{x}_0))d\boldsymbol{x}}{\int_{\boldsymbol{x}\epsilon\chi} d\boldsymbol{x}} = \frac{\int_{\boldsymbol{x}\epsilon\chi} \sigma^2[\boldsymbol{f}(\boldsymbol{x}) - \boldsymbol{f}(\boldsymbol{x}_0)]'(\boldsymbol{X}'\boldsymbol{X})^{-1}[\boldsymbol{f}(\boldsymbol{x}) - \boldsymbol{f}(\boldsymbol{x}_0)]d\boldsymbol{x}}{\int_{\boldsymbol{x}\epsilon\chi} d\boldsymbol{x}}.$$

It can be shown that the average difference variance is proportional to $tr[(\boldsymbol{X}'\boldsymbol{X})^{-1}\boldsymbol{B}_{I_D}]$,

where

$$\boldsymbol{B}_{I_D} = \frac{\int [\boldsymbol{f}(\boldsymbol{x}) - \boldsymbol{f}(\boldsymbol{x}_0)]'[\boldsymbol{f}(\boldsymbol{x}) - \boldsymbol{f}(\boldsymbol{x}_0)] d\boldsymbol{x}}{\int_{\boldsymbol{x}\epsilon\chi} d\boldsymbol{x}} \tag{2.4}$$

is the $p \times p$ matrix $\boldsymbol{B}$ with the first row and the first column set to zero (de Oliveira et al., 2019). Thus, I_D-optimal design seeks to minimize

$$tr[(\boldsymbol{X}'\boldsymbol{X})^{-1}\boldsymbol{B}_{I_D}].$$

I_DP-Optimality Criterion

The I_DP-optimality criterion is another modified optimality criterion defined by de Oliveira et al. (2019). This criterion minimizes the average width of pointwise confidence intervals for the difference in mean response over the entire design region, that is, I_DP-optimal design minimizes

$$tr[(\boldsymbol{X}'\boldsymbol{X})^{-1}\boldsymbol{B}_{I_D}]F_{1,d;1-\alpha}.$$

2.2 Bayesian Optimality Criteria

While designing experiments, it is crucial to ensure that the obtained data can lead to gain insights about an underlying process. Bayesian optimal experimental design happens to be the consolidated approach that addresses this issue by incorporating prior information regarding the statistical model with a design criterion. The design criterion describes the worth of selecting any design

from the design space, yielding data from a sample space. This mathematical framework is based on a decision theoretic approach to experimental design introduced by Lindley (1972).

Bayesian D-Optimality Criterion

In order to eradicate the issue of dependency on model assumption in the classical method, DuMouchel and Jones (1994) provided a modified Bayesian D-criterion that entails the categorization of model terms into primary and potential terms.

Let us consider the partition of a classical linear model as:

$$\boldsymbol{y} = \boldsymbol{X}_1\boldsymbol{\beta}_1 + \boldsymbol{X}_2\boldsymbol{\beta}_2 + \boldsymbol{\epsilon},$$

where $\boldsymbol{X}_1$ is the $n \times p_1$ matrix of primary terms which are assumed as active, $\boldsymbol{\beta}_1$ is the $p_1 \times 1$ vector of parameters for primary terms, $\boldsymbol{X}_2$ is the $n \times p_2$ matrix of potential terms which may or may not be active, and $\boldsymbol{\beta}_2$ is the $p_2 \times 1$ vector of parameters for potential terms. It is to be noted that $p_1 + p_2 = p$.

The effects associated with the primary terms are presumed to have an arbitrary prior mean and a prior variance tending towards infinity owing to the active status of the primary terms. Hence, $\boldsymbol{\beta}_1 \sim N(\mathbf{0}_{p_1}, \gamma^2\sigma^2\boldsymbol{I}_{\boldsymbol{p_1}})$, where $\gamma^2 \to \infty$. While on the other hand, as the potential terms may or may not be active, hence effects associated with the potential terms are presumed to have

a prior mean of zero and a finite prior variance. Thus, $\boldsymbol{\beta}_2 \sim N(\mathbf{0}_{p_2}, \tau^2\sigma^2\boldsymbol{I}_{\boldsymbol{p_2}})$, where $\tau^2\sigma^2$ is a finite prior variance and τ^2 is a predefined value. In this thesis, we assume $\tau^2 = 3$ because we applied our proposed graphical technique on Bayesian optimal designs obtained by Basnayake (2019), where $\tau^2 = 3$ is considered.

The joint prior distribution of the unknown parameters obtained from the combination of $\boldsymbol{\beta}_1$ and $\boldsymbol{\beta}_2$ is $\boldsymbol{\beta}|\sigma^2 \sim N(\mathbf{0}, \sigma^2\boldsymbol{R}^{-1})$, where

$$\boldsymbol{R}^{-1} = \begin{bmatrix} \gamma^2\boldsymbol{I}_{p_1\times p_1} & \mathbf{0}_{p_1\times p_2} \\ \mathbf{0}_{p_2\times p_1} & \tau^2\boldsymbol{I}_{p_2\times p_2} \end{bmatrix}$$

and $\boldsymbol{R} = \boldsymbol{K}/\tau^2$. When $\gamma^2 \to \infty$, $\boldsymbol{K} = \begin{bmatrix} \mathbf{0}_{p_1\times p_1} & \mathbf{0}_{p_1\times p_2} \\ \mathbf{0}_{p_2\times p_1} & \boldsymbol{I}_{p_2\times p_2} \end{bmatrix}$. Assume the conditional distribution of $\boldsymbol{y}$ given $\boldsymbol{\beta}$ and σ^2 is

$$\boldsymbol{y}|(\boldsymbol{\beta}, \sigma^2) \sim N(\boldsymbol{X}\boldsymbol{\beta}, \sigma^2\boldsymbol{I}).$$

Then the posterior distribution for $\boldsymbol{\beta}$ given $\boldsymbol{y}$ is

$$\boldsymbol{\beta}|\boldsymbol{y} \sim N((\boldsymbol{X}'\boldsymbol{X} + \boldsymbol{R})^{-1}\boldsymbol{X}'\boldsymbol{y}, \sigma^2(\boldsymbol{X}'\boldsymbol{X} + \boldsymbol{R})^{-1}). \tag{2.5}$$

The initial objective of the Bayesian D-optimality is to minimize the variance of the parameter estimates, by alleviating the dependency on model assumption. Hence a Bayesian D-optimal design maximizes

$$|\boldsymbol{X}'\boldsymbol{X} + \boldsymbol{R}|.$$

Bayesian DP-Optimality Criterion

In order to obtain partially replicated design, Leonard and Edwards (2017) incorporated the idea of Gilmour and Trinca (2012) and modified the Bayesian D-optimality criterion. They proposed the Bayesian DP-optimality criterion which attempts to maximize

$$\frac{|\boldsymbol{X}'\boldsymbol{X}+\boldsymbol{R}|}{(F_{p,d;1-\alpha})^p}.$$

Bayesian I-Optimality Criterion

From Equation (2.5) we know $Var(\boldsymbol{\beta}|\boldsymbol{y})$ is $\sigma^2(\boldsymbol{X}'\boldsymbol{X}+\boldsymbol{R})^{-1}$. Hence, combining it with Equation (2.1), we get

$$Var(\hat{y}(\boldsymbol{x})) = \sigma^2\boldsymbol{f}'(\boldsymbol{x})(\boldsymbol{X}'\boldsymbol{X}+\boldsymbol{R})^{-1}\boldsymbol{f}(\boldsymbol{x})). \tag{2.6}$$

It follows that the average prediction variance is

$$\frac{\int_{\boldsymbol{x}\epsilon\chi} Var(\hat{\boldsymbol{y}}(x))d\boldsymbol{x}}{\int_{\boldsymbol{x}\epsilon\chi} d\boldsymbol{x}} = \frac{\int_{\boldsymbol{x}\epsilon\chi} \sigma^2\boldsymbol{f}'(\boldsymbol{x})(\boldsymbol{X}'\boldsymbol{X}+\boldsymbol{R})^{-1}\boldsymbol{f}(\boldsymbol{x})d\boldsymbol{x}}{\int_{\boldsymbol{x}\epsilon\chi} d\boldsymbol{x}}$$

$$\propto \int_{\boldsymbol{x}\epsilon\chi} \boldsymbol{f}'(\boldsymbol{x})(\boldsymbol{X}'\boldsymbol{X}+\boldsymbol{R})^{-1}\boldsymbol{f}(\boldsymbol{x})d\boldsymbol{x}.$$

As $\boldsymbol{f}'(\boldsymbol{x})(\boldsymbol{X}'\boldsymbol{X}+\boldsymbol{R})^{-1}\boldsymbol{f}(\boldsymbol{x})$ is a scaler, we can write,

$$\boldsymbol{f}'(\boldsymbol{x})(\boldsymbol{X}'\boldsymbol{X}+\boldsymbol{R})^{-1}\boldsymbol{f}(\boldsymbol{x}) = tr(\boldsymbol{f}'(\boldsymbol{x})(\boldsymbol{X}'\boldsymbol{X}+\boldsymbol{R})^{-1}\boldsymbol{f}(\boldsymbol{x})).$$

By cyclically permuting matrices, we can write

$$tr(\boldsymbol{f}'(\boldsymbol{x})(\boldsymbol{X}'\boldsymbol{X}+\boldsymbol{R})^{-1}\boldsymbol{f}(\boldsymbol{x})) = tr((\boldsymbol{X}'\boldsymbol{X}+\boldsymbol{R})^{-1}\boldsymbol{f}(\boldsymbol{x})\boldsymbol{f}'(\boldsymbol{x})).$$

It follows that

$$\begin{aligned}\int_{\boldsymbol{x}\epsilon\chi} \boldsymbol{f}'(\boldsymbol{x})(\boldsymbol{X}'\boldsymbol{X}+\boldsymbol{R})^{-1}\boldsymbol{f}(\boldsymbol{x})d\boldsymbol{x} &= \int_{\boldsymbol{x}\epsilon\chi} tr[(\boldsymbol{X}'\boldsymbol{X}+\boldsymbol{R})^{-1}\boldsymbol{f}(\boldsymbol{x})\boldsymbol{f}'(\boldsymbol{x})]d\boldsymbol{x} \\ &= tr[\int_{\boldsymbol{x}\epsilon\chi} (\boldsymbol{X}'\boldsymbol{X}+\boldsymbol{R})^{-1}\boldsymbol{f}(\boldsymbol{x})\boldsymbol{f}'(\boldsymbol{x})d\boldsymbol{x}] \\ &= tr[(\boldsymbol{X}'\boldsymbol{X}+\boldsymbol{R})^{-1}\int_{\boldsymbol{x}\epsilon\chi} \boldsymbol{f}(\boldsymbol{x})\boldsymbol{f}'(\boldsymbol{x})d\boldsymbol{x}].\end{aligned}$$

By (2.3) the average prediction variance is proportional to $tr[(\boldsymbol{X}'\boldsymbol{X}+\boldsymbol{R})^{-1}\boldsymbol{B}]$. Bayesian I-optimal design is defined to minimize the average prediction variance, that is, minimize

$$tr[(\boldsymbol{X}'\boldsymbol{X}+\boldsymbol{R})^{-1}\boldsymbol{B}].$$

Bayesian IP-Optimality Criterion

Basnayake (2019) presented the Bayesian IP-optimality criterion by using the idea in Gilmour and Trinca (2012) and de Oliveira et al. (2019) for selecting partially replicated designs that facilitate inference procedure. This criterion attempts to minimize

$$tr[(\boldsymbol{X}'\boldsymbol{X}+\boldsymbol{R})^{-1}\boldsymbol{B}]F_{1,d;1-\alpha}.$$

Bayesian I_D-Optimality Criterion

Employing the concept of I_D-optimality criterion in Bayesian framework and utilizing Equation (2.5), Basnayake (2019) introduced the Bayesian I_D-optimality criterion that selects partially replicated optimal designs with high prediction efficiency. This criterion seeks to minimize

$$tr[(\boldsymbol{X}'\boldsymbol{X} + \boldsymbol{R})^{-1}\boldsymbol{B}_{I_D}].$$

Bayesian I_DP-Optimality Criterion

Basnayake (2019) also introduced the Bayesian I_DP-optimality criterion for obtaining partially replicated designs with high prediction efficiency that allows the experimenter to conduct formal lack of fit tests. Bayesian I_DP-optimality criterion aims to minimize

$$tr[(\boldsymbol{X}'\boldsymbol{X} + \boldsymbol{R})^{-1}\boldsymbol{B}_{I_D}]F_{1,d;1-\alpha}.$$

2.3 Graphical Assessment Techniques

2.3.1 Variance Dispersion Graph

Introduced by Giovannitti-Jensen and Myers (1989), variance dispersion graph (VDG) is a graphical technique used for the evaluation of the overall prediction properties of an experimental design using scaled predction variance. The

standardized or scaled prediction variance (SPV) for a design ξ_n, at any point $\boldsymbol{x} \in \chi$, is defined as

$$d(\boldsymbol{x}, \xi_n) = \frac{n\, Var(\hat{y}(\boldsymbol{x}))}{\sigma^2}.$$

By (2.1), we obtain

$$d(\boldsymbol{x}, \xi_n) = \frac{n\, \sigma^2 \boldsymbol{f}'(\boldsymbol{x})(\boldsymbol{X}'\boldsymbol{X})^{-1}\boldsymbol{f}(\boldsymbol{x})}{\sigma^2}$$

$$= n\, \boldsymbol{f}'(\boldsymbol{x})(\boldsymbol{X}'\boldsymbol{X})^{-1}\boldsymbol{f}(\boldsymbol{x}). \tag{2.7}$$

Note that $sigma^2$, which is unknown, disappears in (2.7).The rationale for scaling the prediction variance with the number of experimental runs n is to set the criterion on a per observation basis. This leads to a better understanding of the quality of information any design offers. This insights are of remarkabe significance when the experiments are expensive or involves several constraints. For a better understanding of the implications of SPV, we consider the following example.

Example 1

Consider a design ξ_3 with one factor x from the experimental region $\chi = [-1, 1]$ with runs at $1, -1, 0$. Assume the model is

$$\hat{y}(x) = \hat{\beta}_0 + \hat{\beta}_1 x. \tag{2.8}$$

It can be written as

$$\hat{y}(x) = \begin{bmatrix} 1 & x \end{bmatrix} \begin{bmatrix} \hat{\beta}_0 \\ \hat{\beta}_1 \end{bmatrix} = \boldsymbol{f}_1'(x)\hat{\boldsymbol{\beta}}_1, \tag{2.9}$$

where $\boldsymbol{f}_1'(x) = \begin{bmatrix} 1 & x \end{bmatrix}$ and $\hat{\boldsymbol{\beta}}_1 = \begin{bmatrix} \hat{\beta}_0 \\ \hat{\beta}_1 \end{bmatrix}$.

Now, $\boldsymbol{X} = \begin{bmatrix} 1 & 1 \\ 1 & -1 \\ 1 & 0 \end{bmatrix}$. By Equation (2.7), we get that the SPV at x is

$$d_1(x, \xi_3) = 3[\boldsymbol{f}_1'(x) \begin{bmatrix} 3 & 0 \\ 0 & 2 \end{bmatrix}^{-1} \boldsymbol{f}_1(x)]$$

$$= 3(\frac{1}{3} + \frac{1}{2}x^2).$$

Now, if we assume that the model is

$$\hat{y}(x) = \hat{\beta}_0 + \hat{\beta}_1 x + \hat{\beta}_2 x^2, \tag{2.10}$$

which can be written as

$$\hat{y}(x) = \begin{bmatrix} 1 & x & x^2 \end{bmatrix} \begin{bmatrix} \hat{\beta}_0 \\ \hat{\beta}_1 \\ \hat{\beta}_2 \end{bmatrix} = \boldsymbol{f}_2'(\boldsymbol{x})\hat{\boldsymbol{\beta}}_2,$$

where $\boldsymbol{f}_2'(\boldsymbol{x}) = \begin{bmatrix} 1 & x & x^2 \end{bmatrix}$ and $\hat{\boldsymbol{\beta}}_2 = \begin{bmatrix} \hat{\beta}_0 \\ \hat{\beta}_1 \\ \hat{\beta}_2 \end{bmatrix}$. Since $\boldsymbol{X} = \begin{bmatrix} 1 & 1 & 1 \\ 1 & -1 & 1 \\ 1 & 0 & 0 \end{bmatrix}$, the SPV at x is

$$d_2(x, \xi_3) = 3[\boldsymbol{f}_2'(x) \begin{bmatrix} 3 & 0 & 2 \\ 0 & 2 & 0 \\ 2 & 0 & 2 \end{bmatrix}^{-1} \boldsymbol{f}_2(x)]$$

$$= 3(1 - \frac{3}{2}x^2 + \frac{3}{2}x^4).$$

The variance dispersion graph is a two dimensional graph where the x-axis represents the radii of the design region. The graph portrays the maximum, minimum and average prediction variances over the entire design region. A proportinately flat VDG, with the maximum and minimum SPV curve digressing less from the average SPV curve is preferable and considered as stable SPV. Let $U_r = \{\boldsymbol{x} : \boldsymbol{x}'\boldsymbol{x} = r^2\}$ be the surface of a hypersphere of radius r centred at the orgin of the design space. The spherical average of the scaled prediction variance is defined as

$$V^r = \frac{n\,\Psi \int_{U_r} Var(\hat{y}(\boldsymbol{x}))d\boldsymbol{x}}{\sigma^2},$$

which is the average of the variances of the estimated responses over the surface of the sphere.

It can be shown that

$$V^r = n\,tr[(\boldsymbol{X}'\boldsymbol{X})^{-1}\boldsymbol{S}], \tag{2.11}$$

where

$$\boldsymbol{S} = \Psi \int_{U_r} \boldsymbol{f}(\boldsymbol{x})\boldsymbol{f}'(\boldsymbol{x})d\boldsymbol{x} \tag{2.12}$$

is a $p \times p$ matrix of spherical region moments of the hypersphere U_r and $\Psi^{-1} = \int_{U_r} d\boldsymbol{x}$ is the surface area of U_r. Hussey et al. (1987) used Equation (2.11) for the evaluation of response surface designs for simulation models. Note

that $\boldsymbol{S} = \boldsymbol{B}$ when the design space is spherical region. Giovannitti-Jensen and Myers (1989) showed that each entry of $\boldsymbol{S}$ has the form

$$\sigma_{\delta_1,\delta_2,\ldots,\delta_m} = \Psi \int_{U_r} x_1^{\delta_1} x_2^{\delta_2} \ldots x_m^{\delta_m} d\mathbf{x}.$$

Since the surface of the hypershpere U_r is symmetric, if any of the δ_i is odd, then $\sigma_{\delta_1,\delta_2,\ldots,\delta_m}$ is zero. When all the elements of δ_i are even, then (Schoonees et al., 2016)

$$\sigma_{\delta_1,\delta_2,\ldots,\delta_m} = \frac{r^{\sum_1^m \delta_i} \Gamma(\frac{m}{2}) \prod_{i=1}^m \Gamma(\frac{\delta_i+1}{2})}{\pi^{\frac{m}{2}} \Gamma(\frac{\sum_1^m \delta_i + m}{2})}. \tag{2.13}$$

The variance dispersion graph for a 24-run I-optimal design provided in Table 2.1 is displayed in Figure 2.1. We observe that the range of the radii is from 0 to 1.732. The maximum, minimum and average SPV curve start out low (close to zero) at the origin and as the distance from the origin increases, the deviation between the three curves appears prominently. The highest value of the maximum SPV curve is 39.706 (the value is obtained from R output), which appears at the design perimeter with radius 1.732, where the highest value of the average SPV also occurs with value 21.280. The highest SPV value for the minimum SPV curve is also at the perimeter, which is 8.90. The minimum SPV is 2.855 which occurs when the radius is around 1.0. We can conclude from this graph that the I-optimal design has relatively stable SPV up to radius 1.0 but tends to have fluctuating SPV near the peripheral region.

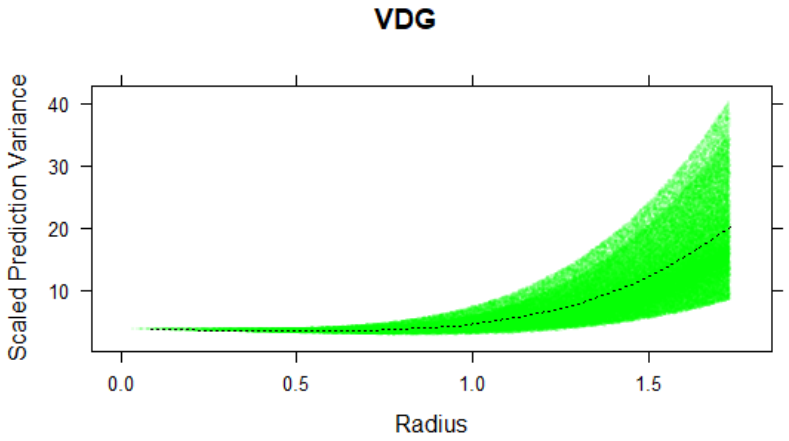

Figure 2.1: VDG for the 24-run I-optimal design in Table 2.1

2.3.2 Quantile Plot

Based on the same methodology as VDG, the quantile plot was presented by Khuri et al. (1996) which contains more information about the distribution of the SPV over the hyperspheres. Two designs with simliar VDGs might have different SPV distributions. In such situations, quantile plots turns out to be an effective tool for distinction between the two designs. Each curve in this plot represents the emperical cumulative distribution of the SPV over each hypersphere.

The methodology employed in quantile plot is to randomly sample a large number of points n^* on the surface of each hypersphere. Let d_i^r be the SPV calculated at the i^{th} sampled point and d_{i,n^*}^r be the i^{th} smallest value of the SPV. Assuming that there are no ties, the SPV values are ordered as d_i^r's

in the following way:

$$d^r_{1,n^*} < d^r_{2,n^*} < ... < d^r_{n^*,n^*}.$$

Then the emperical cumulative distribution function(or ecdf) of the SPV over the hypersphere of radius r, denoted by $\hat{F}_n.(d)$, is estimated as:

$$\hat{F}_n.(d) = \frac{\sum_{i=1}^{n^*} I(d^r_i \leq d)}{n^*} = \frac{i}{n} \text{ if } d \in \left[d^r_{i,n^*}, d^r_{i+1,n^*}\right), \tag{2.14}$$

where $I(.)$ is the indicator function. Hence, a weight of $1/n^*$ is allotted to each SPV value. Equation (2.14) also holds when there are tied values, by summing up the weights. The quantile plots are obtained by employing linear interpolation at different radii and their respective ecdf's are displayed in each plot. The x-axis of the quantile plot represents the quantiles corresponding to the SPV distribution for each specific radius. For example, $p = 0$, 0.5 and 1 represent the quantiles corresponding to the minimum, median and maximum of the SPV distribution, respectively.

Figure 2.2 contains an illustration of quantile plot for the I-optimal design in Table 2.1 at 20 different radii. For example when the radius is 1.299, the SPV value 10 appears at the 80^{th} percentile, whereas at radius 1.472 and 1.559, it is at the 40^{th} and 20^{th} percentile, respectively. When the radius is less than or equal to 1.126, the graphs depict that all the SPVs are distributed below 10.

According to Box and Hunter (1957) rotatable designs refer to the de-

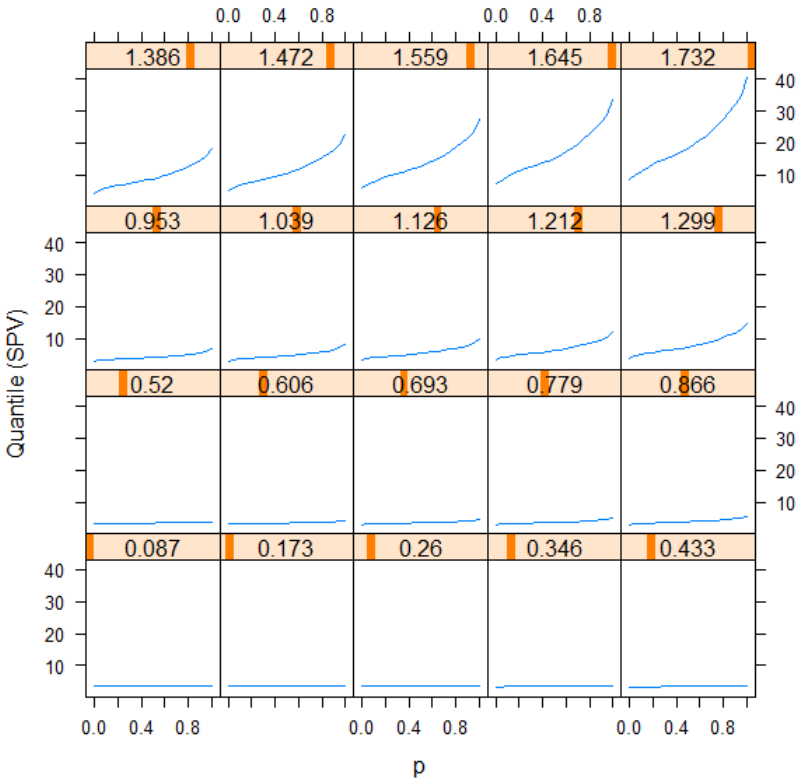

Figure 2.2: Quantile plot for the 24-run I-optimal design in Table 2.1

signs where estimated response has a constant variance at all points which have the same distance from the centre of the design, thus ensuring a stable prediction variance over the entire experimental region. From Figure 2.2, we can see that up to radius is approximately 0.95, the SPV values are more or less stable over the hypersphere and, thus, the design is nearly rotatable. Beyond that point the SPV values start increasing rapidly and the curve tends to be steeper, where the I-optimal design is not rotatable anymore.

2.3.3 Fraction of Design Space Plots

The VDG assigns equal weight to the SPV for all radii, which is a vital limitation of this technique. This weighting issue is addressed in the fraction of design space (FDS) plot by taking an account of the volume of the design region represented by the hypersphere of each radius. Hence, it is crucial to use both FDS plot and VDG together as it is not always known in advance where in the design space predictions will need to be made. The FDS plot aims to procure a design that can provide accurate prediction over the whole design region.

Let ψ be the total volume of the design region, υ be any specific value of SPV, $A = \{(\boldsymbol{x} = x_1, x_2, ..., x_m) : \upsilon(\boldsymbol{x}) < \upsilon\}$, where $\upsilon(\boldsymbol{x})$ represents SPV at $\boldsymbol{x}$. Zahran et al. (2003) defined the FDS-criterion as

$$FDS(\upsilon) = \frac{1}{\psi} \int_A d\boldsymbol{x}. \tag{2.15}$$

Since the elements in A are usually unknown, we rewrite (2.15) as an integral over the whole design region by utilizing an indicator function $I(\boldsymbol{x}) \in \{0, 1\}$ such that

$$I(\boldsymbol{x}) = \begin{cases} 0.5^{\frac{|g(\boldsymbol{x})|-g(\boldsymbol{x})}{g(\boldsymbol{x})}}, & g(\boldsymbol{x}) \neq 0 \\ \\ 0, & g(\boldsymbol{x}) = 0 \end{cases},$$

where $g(\boldsymbol{x}) = \upsilon(\boldsymbol{x}) - \upsilon$. Therefore, A can be defined as $A = \{(x_1, x_2 ... x_m) : g(\boldsymbol{x}) < 0\}$. Now (2.15) can be written as

$$FDS(\upsilon) = \frac{1}{\psi} \int_{\chi} I(\boldsymbol{x}) d\boldsymbol{x},$$

which can be computed using a multivariate numerical integration routine. The FDS plot displays FDS(υ) versus υ for each value of υ. A relatively flatter curve depicts that the SPV does not vary a lot over the design region.

Figure 2.3 provides the FDS plot for the I-optimal design in Table 2.1. The FDS plot of the I-optimal design in Figure 2.3 does not indicate where in the design region the maximum or the minimum value occurs unlike the VDG plot. However, from the FDS plot, we can see the fraction of the design space for which the SPV value is less than or equal to a given value, which cannot been seen from the VDG. For example, if we consider the SPV value 10, the corresponding value in the x-axis is 0.6, which indicates that 60% of the entire design space has SPV value less than or equal to 10.

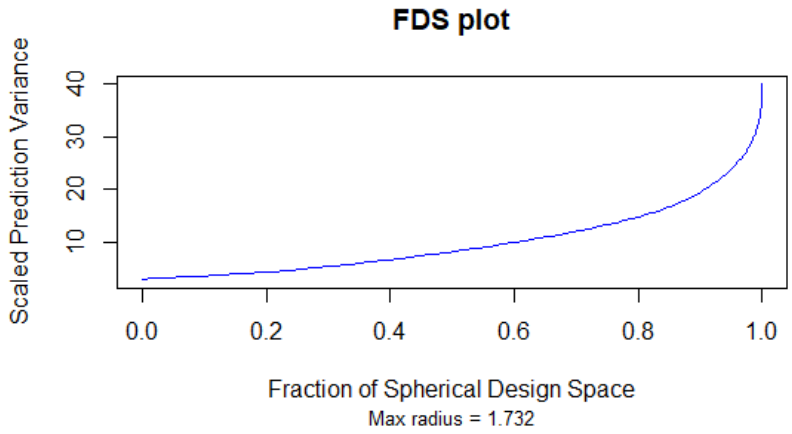

Figure 2.3: FDS plot for 24-run I-optimal design in Table 2.1

2.3.4 Variance Ratio Fraction of Design Space Plot

An updated version of the FDS plot is the variance ratio FDS plot (or VRFDS). This plot is useful when a couple of designs need to be compared to a reference design. Unlike the FDS plot, a VRFDS plot is then constructed by using the log ratio of the SPV of the specific design to the SPV of the reference design.

Let ξ_1 and ξ_2 be the reference design and design of interest respectively. Then, for the randomly simulated point $\boldsymbol{x}^*$, the log variance ratio is

$$logVR(\boldsymbol{x}^*, \xi_2, \xi_1) = log\frac{d(\boldsymbol{x}^*, \xi_2)}{d(\boldsymbol{x}^*, \xi_1)}.$$

The mechanism for this plot is similar to the SPV algorithm. After the calculation of log variance ratio for each simulated points, they are ranked in ascending order and plotted against $\frac{0}{n}, \frac{1}{n}, ..., \frac{n-1}{n}$. The plot facilitates comparison of both

high and low variance ratios directly. Hence, the y-axis in this plot represents log ratio of the SPV and the x-axis represents the fraction of the total design space. In this plot, the reference design is represented by a horizontal line as it will have a constant variance ratio. Based on this plot, a design is preferable if the variance ratio for the design is less than one, since it indicates that the design has a lower SPV than the reference design. A design that yields better predictions over much of the experimental region will have a relatively larger portion of the curve below the horizontal line representing the reference design.

Chapter 3

Graphs for Bayesian Designs

The existing graphical techniques like VDG, FDS plot, quantile plot and VRFDS plot are not applicable for the assessment of Bayesian designs. In this chapter, we propose a modification of such graphs which allows the assessment of Bayesian optimal designs. This modification is based on the calculation of the standardized or scaled prediction variance (SPV) for the Bayesian designs. We consider the second order models, where we main effects and quadratic effects are primary terms and the two-factor interactions are potential terms.

Section 3.1 presents the derivation of SPV and average SPV for Bayesian designs. Section 3.2 describes the algorithms for obtaining the graphs for the assessment of Bayesian designs. Section 3.3 provide the VDGs and FDS plots for 24-run 3-level Bayesian optimal designs with 3 factors tabulated in Basnayake (2019). The same graphs for 30-run 3-level Bayesian optimal designs with 4 factors in Basnayake (2019) are obtained in section 3.4.

3.1 SPV and Average SPV of Bayesian Designs

By (2.6), the variance of the predicted response at some $\boldsymbol{x}$ in the design region is given by $Var(\hat{y}(x)) = \sigma^2 \boldsymbol{f}'(\boldsymbol{x})(\boldsymbol{X}'\boldsymbol{X} + \boldsymbol{R})^{-1}\boldsymbol{f}(\boldsymbol{x})$. Now, for a Bayesian design ξ_n, the standardized or scaled prediction variance (SPV) is defined as

$$\begin{aligned} d(x, \xi_n) &= \frac{n\, Var(\hat{y}(\boldsymbol{x}))}{\sigma^2} \\ &= \frac{n\, \sigma^2 \boldsymbol{f}'(\boldsymbol{x})(\boldsymbol{X}'\boldsymbol{X} + \boldsymbol{R})^{-1}\boldsymbol{f}(\boldsymbol{x})}{\sigma^2} \\ &= n\, \boldsymbol{f}'(\boldsymbol{x})(\boldsymbol{X}'\boldsymbol{X} + \boldsymbol{R})^{-1}\boldsymbol{f}(\boldsymbol{x}). \end{aligned} \tag{3.1}$$

Example 2

Consider the design in Example 1 and assume the model is (2.10) with the primary terms being 1 and x and the potential term being x^2. Thus, $p_1 = 2$ and $p_2 = 1$. Considering $\tau^2 = 1$, we get the prior covariance matrix $\mathbf{R} = \mathbf{K}$ where

$$\mathbf{K} = \begin{bmatrix} 0 & 0 & 0 \\ 0 & 0 & 0 \\ 0 & 0 & 1 \end{bmatrix}.$$

Now, utilizing Equation (3.1) we get

$$d(x,\xi_3) = 3[\boldsymbol{f}'(\boldsymbol{x})(\begin{bmatrix}3&0&2\\0&2&0\\2&0&2\end{bmatrix}+\mathbf{R})^{-1}\boldsymbol{f}(\boldsymbol{x})]$$

$$= 3[\boldsymbol{f}'(\boldsymbol{x})(\begin{bmatrix}3&0&2\\0&2&0\\2&0&2\end{bmatrix}+\begin{bmatrix}0&0&0\\0&0&0\\0&0&1\end{bmatrix})^{-1}\boldsymbol{f}(\boldsymbol{x})]$$

$$= 3(\frac{3}{5}-\frac{3}{10}x^2+\frac{3}{5}x^4).$$

For any $\boldsymbol{x}$ in U_r, the average SPV is defined as

$$V^r = \frac{n\,\Psi\int_{U_r} Var(\hat{y}(\boldsymbol{x}))d\boldsymbol{x}}{\sigma^2}$$

$$= n\,\Psi\int_{U_r}\boldsymbol{f}'(\boldsymbol{x})(\boldsymbol{X}'\boldsymbol{X}+\boldsymbol{R})^{-1}\boldsymbol{f}(\boldsymbol{x})d\boldsymbol{x}$$

$$= n\,\Psi\int_{U_r} tr[\boldsymbol{f}'(\boldsymbol{x})(\boldsymbol{X}'\boldsymbol{X}+\boldsymbol{R})^{-1}\boldsymbol{f}(\boldsymbol{x})]d\boldsymbol{x}$$

$$= n\,\Psi tr[\int_{U_r}(\boldsymbol{X}'\boldsymbol{X}+\boldsymbol{R})^{-1}\boldsymbol{f}(\boldsymbol{x})\boldsymbol{f}'(\boldsymbol{x})d\boldsymbol{x}]$$

$$= n\,\Psi tr[(\boldsymbol{X}'\boldsymbol{X}+\boldsymbol{R})^{-1}\int_{U_r}\boldsymbol{f}(\boldsymbol{x})_{\boldsymbol{f}'(\boldsymbol{x})}d\boldsymbol{x}]$$

$$= n\,tr[(\boldsymbol{X}'\boldsymbol{X}+\boldsymbol{R})^{-1}\boldsymbol{S}] \tag{3.2}$$

by (2.12). In this thesis, for the generation of VDGs, FDS plots and quantile plots, spherical design region is considered. In section 3.3 and section 3.4, SPV and average SPV are calculated using (3.1) and (3.2) for Bayesian I-optimal

and Bayesian D-optimal designs. The existing methodology applied to the graphs remains unchanged.

For Bayesian IP-optimal design, the SPV and the average SPV are calculated using

$$d(x, \xi_n) = n\, \boldsymbol{f}'(\boldsymbol{x})(\boldsymbol{X}'\boldsymbol{X} + \boldsymbol{R})^{-1}\boldsymbol{f}(\boldsymbol{x})F_{1,d;1-\alpha} \tag{3.3}$$

and

$$V^r = n\, tr[(\boldsymbol{X}'\boldsymbol{X} + \boldsymbol{R})^{-1}\boldsymbol{S}]F_{1,d;1-\alpha}, \tag{3.4}$$

respectively.

For Bayesian DP-optimal design, the corresponding formulas are

$$d(x, \xi_n) = n\, \boldsymbol{f}'(\boldsymbol{x})(\boldsymbol{X}'\boldsymbol{X} + \boldsymbol{R})^{-1}\boldsymbol{f}(\boldsymbol{x})(F_{p,d;1-\alpha})^p \tag{3.5}$$

and

$$V^r = n\, tr[(\boldsymbol{X}'\boldsymbol{X} + \boldsymbol{R})^{-1}\boldsymbol{S}](F_{p,d;1-\alpha})^p, \tag{3.6}$$

respectively.

Similarly, for Bayesian I_D-optimal design we compute

$$d(x, \xi_n) = n\, \boldsymbol{f}'(\boldsymbol{x})(\boldsymbol{X}'\boldsymbol{X} + \boldsymbol{R})^{-1}\boldsymbol{f}(\boldsymbol{x}) \tag{3.7}$$

and replace the first row and first column by zero to obtain the SPVs. Let $\boldsymbol{S}_D$ be the $\boldsymbol{S}$ matrix with the first row and first column replaced by zero, then the average SPV is computed by

$$V^r = n\, tr[(\boldsymbol{X}'\boldsymbol{X} + \boldsymbol{R})^{-1}\boldsymbol{S}_D]. \tag{3.8}$$

Lastly, the SPV and the average SPV for Bayesian I_DP-optimal design can be calculated by

$$d(x, \xi_n) = n\, \boldsymbol{f}'(\boldsymbol{x})(\boldsymbol{X}'\boldsymbol{X} + \boldsymbol{R})^{-1}\boldsymbol{f}(\boldsymbol{x})F_{1,d;1-\alpha} \tag{3.9}$$

and

$$V^r = n\, tr[(\boldsymbol{X}'\boldsymbol{X} + \boldsymbol{R})^{-1}\boldsymbol{S}_D]F_{1,d;1-\alpha}, \tag{3.10}$$

respectively.

3.2 Generation of Graphs with Random Sampling Approach

Following Schoonees et al. (2016), we employed Monte Carlo simulation for randomly sampling approach. The spherical multivariate normal distribution is used for random sampling over the required hypersphere. The mechanism for the generation of VDG is highlighted in the following steps.

1. Sample a large number of points directly and uniformly from a normal distribution over the required hypersphere.

2. Calculate SPV at each of the sampled points using Equation (3.1).

3. Calculate the average SPV applying Equation (3.2).

4. Determine the distance of each sampled point to the origin

5. Plot the SPV and average SPV against the distance for each point.

The quantile plots also follows the same mechanism as VDG, therefore similar steps are also implemented for the generation of quantile plots for the evaluation of Bayesian optimal designs. For each specific radius

1. Sample a large number of points directly and uniformly from a normal distribution over the required hypersphere.

2. Calculate SPV at each of the sampled points using Equation (3.1) and arrange them in ascending order.

3. Compute the ecdf $\hat{F}_n.(d)$ of the SPV using Equation (2.14). Sum up the weights if tied values occur.

4. Plot the estimates of ecdfs against the sorted SPVs.

In FDS plot, for the calculation of FDS criterion, Zahran et al. (2003) intially suggested employing 'a fine grid' of points. While Borkowski (2003) argued that Monte Carlo method for random sampling yields significantly accurate results than grid points, with smaller number of randomly generated points. Subsequently, the use of Monte Carlo sampling method was preferred for FDS plot instead of grid points (Goldfarb et al., 2004 and Ozol-Godfrey, 2004). In this study, we used the random sampling approach for FDS plot construction.

1. First, sample a large number of points directly and uniformly from a normal distribution over the required hypersphere.

2. Calculate SPV at each of the sampled points of the design using equation (3.1).

3. Compute approximate value of the FDS criterion using the proportion of points that have SPV value lower than υ.

4. Plot the values of FDS(υ) against υ.

The methodology for VRFDS plot remains the same for the Bayesian optimal designs, apart from the calculation of SPV.

We have adopted and modified the R codes from R package *vdg* (Schoonees et al., 2016) to obtain the graphs for Bayesian designs. When the sampled points are large enough to sufficiently cover the experimental region, the obtained graph yields conspicuous information on the spread of the SPV over concentric hyperspheres. This way, we circumvented the optimiztion problem for finding exact minimum and maximum SPV curve. Ideally, in case of 4 or fewer design factors, the number of Monte Carlo simulations recommended is 2000 to 5000 (Ozol-Godfrey, 2004). The two cases we have considered have 3 and 4 design factors, respectively. Thus, the number of randomly generated points used in this thesis is 5000.

3.3 VDGs and FDS Plots for 24-Run 3-Factor Bayesian Optimal Designs

In this section, we provide the VDGs and FDS plots for 24-run 3-factor Bayesian I-, D-, IP-, DP-, I_D- and I_DP-optimal designs. The scaled prediction variances and the average prediction variances in the VDGs and FDS plots of the Bayesian optimal designs are computed using the corresponding formulas in section 3.2.

Figure 3.1 provides the VDGs for the six Bayesian optimal designs. The range of the radius is from 0 to 1.732. The maximum, minimum and average SPV curves of all the Bayesian designs start out low near the origin, and increase near the perimeter. The highest SPV values of the maximum, average and minimum SPV curves of Bayesian I-optimal design are approximately 44, 26 and 13, respectively. Corresponding values for Bayesian D-optimal design are close to 56, 30 and 10, respectively. The SPV values for Bayesian DP-optimal design are excessively large owing to the F-value being multiplied. From the VDGs of Bayesian IP- , I_D- and I_DP designs, we can observe that the maximum and minimum SPV curves deviate less from the average SPV curve.

Figure 3.2 displays the FDS plots for the six Bayesian optimal designs. Although, a design with low and comparatively flat FDS plot is preferrable, a curve starting out low on the left of the plot evidently depicts that the

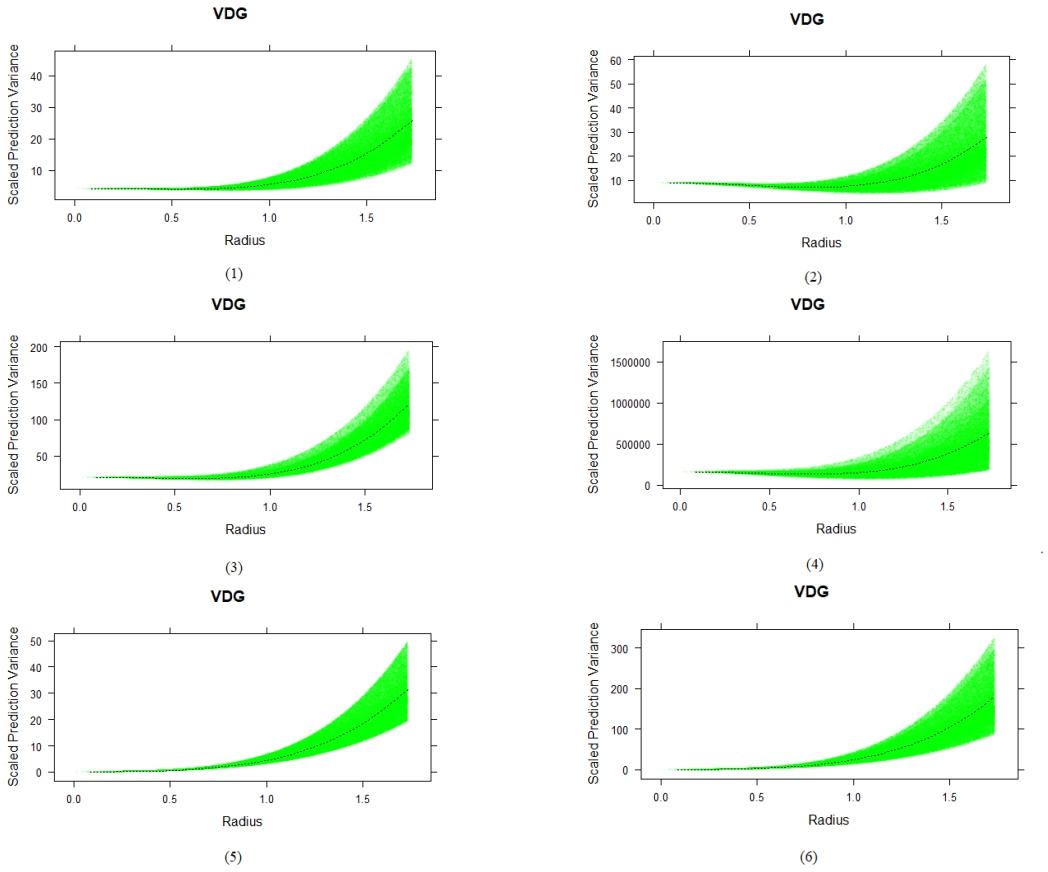

Figure 3.1: VDGs for 24-run Bayesian (1) I- (2) D- (3) IP- (4) DP- (5) I_D- and (6) I_DP-optimal designs

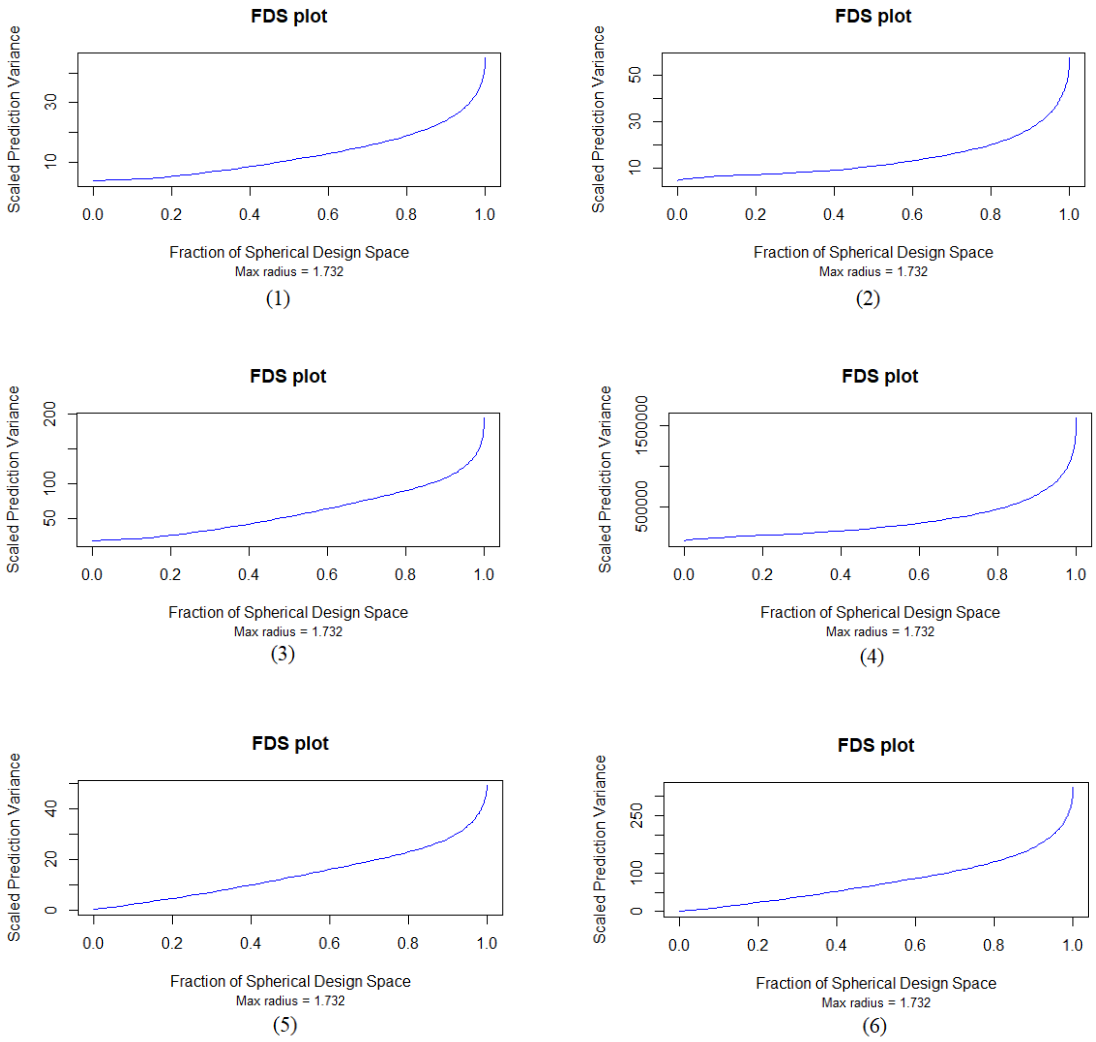

Figure 3.2: FDS plots for 24-run Bayesian (1) I- (2) D- (3) IP- (4) DP- (5) I_D- and (6) I_DP-optimal designs

design yields relatively smaller and less fluctuating SPV values over at least a small fraction of the total design space. Therefore, from the FDS plots of the Bayesian optimal designs, we can conclude that all these designs have comparatively stable and unvarying SPV values for at least 20% to 40% of the total design space. For Bayesian I-optimal design, in approximately 80% of the design space, the SPV values are less than or equal than 20. The FDS plots of Bayesian DP- and D-optimal designs illustrate that the designs have respectively less fluctuating SPV values for about 80% of the design space. We can observe that FDS plot is steeper for Bayesian IP- and I_D-optimal designs, revealing that the difference between the minimum and maximum SPV values is greater in 60% of the design space for these two designs where relatively large SPV values occur.

3.4 VDGs and FDS Plots for 30-Run 4-Factor Bayesian Optimal Designs

In this section, we will provide the VDGs and FDS plots for 30-run 4-factor Bayesian I-, D-, IP-, DP-, I_D- and I_DP-optimal designs. Figure 3.3 provides the VDGs for the six Bayesian optimal designs. The range of the radius is from 0 to 2.0. From the VDGs we can see that the all the designs have their minimum, maximum and average SPV curves at a relatively lower position near the origin up to radius 1.0, and increase after that point. The highest SPV values of the maximum, average and minimum SPV curves of Bayesian

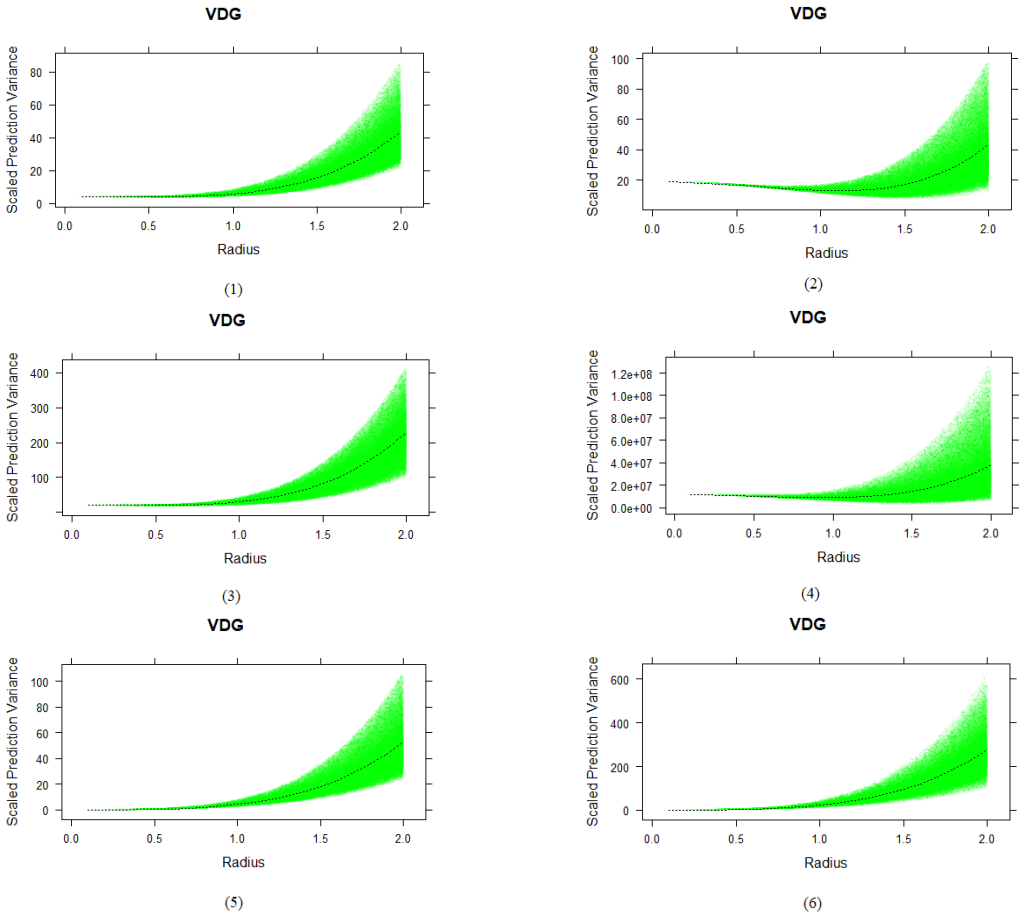

Figure 3.3: VDGs for 30-run Bayesian (1) I- (2) D- (3) IP- (4) DP- (5) I_D- and (6) I_DP-optimal designs

I-optimal design are approximately 84, 42 and 25, respectively. For Bayesian D-optimal design the highest SPV values of the maximum and average SPV curve occur near the perimeter, which are close to 97 and 41, respectively. But the maximum value of the minimum SPV curve occurs near the origin, which is approximately 20. The SPV values for Bayesian DP-optimal design are excessively large due to the F-value being considered but the minimum, maximum and average SPV curves have a similar pattern to that of Bayesian D-optimal designs. The maximum and minimum SPV curves of Bayesian IP- , Bayesian I_D- and Bayesian I_DP-optimal designs digress less from their respective average SPV curves.

Figure 3.4 displays the FDS plots for the six Bayesian optimal designs. From the FDS plot of Bayesian I-optimal design, we can observe that at SPV value 20, the corresponding value in the x-axis is approximately 0.43, meaning 43% of the total design space has SPV values less than or equal to 20. Bayesian D-optimal design seems to have a relatively flatter curve when the total design space is less than 60%. Although, the SPV values are excessively high for Bayesian DP-optimal design, it has flatter FDS curve for approximately 80% of the total design space, signifying less fluctuation in the SPV values for most of the design space. The FDS plots are steeper for Bayesian IP- and I_D-optimal designs, which indicates that these two designs have more fluctuating SPV values. From the FDS plot of Bayesian I_DP-optimal design we can surmise that it has less fluctuating SPV values for approximately 30% of the total design space.

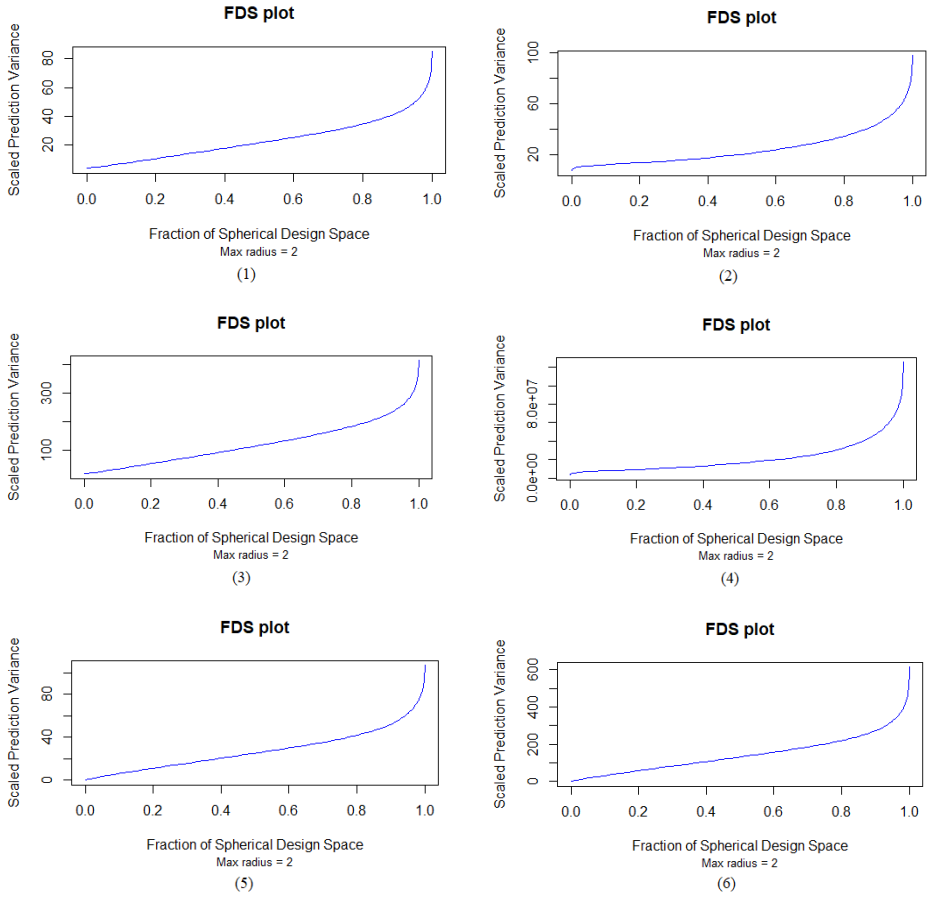

Figure 3.4: FDS plots for 30-run Bayesian (1) I- (2) D- (3) IP- (4) DP- (5) I_D- and (6) I_DP-optimal designs

Chapter 4

Comparison of Bayesian Optimal Designs with Bayesian I-Optimal Design

In this chapter, we will compare Bayesian optimal designs with Bayesian I-optimal design. The scaled prediction variance and the average SPV are computed by the formulas (3.1) and (3.2), respectively. The model consists of main and quadratic effects along with two-factor interaction effects. The main effects and the second order effects are considered as active effects and the two-factor interactions are considered as potential effects.

In section 4.1, we compare 24-run 3-factor Bayesian optimal designs with the Bayesian I-optimal design in Table A.1 and Table A.2. Section 4.2 contains the comparison of 30-run 4-factor Bayesian optimal designs with Bayesian I-optimal design in Table A.3, Table A.4 and Table A.5.

4.1 24-Run 3-Factor Bayesian Optimal Designs

In this section, we will compare 24-run 3-factor Bayesian optimal designs using the variance dispersion graphs and the fraction of design space plots. Quantile plots, boxplots, and the variance ratio FDS plots will also be used to compare some of the designs.

Figure 4.1 contains the VDG and FDS plot for Bayesian I- and Bayesian

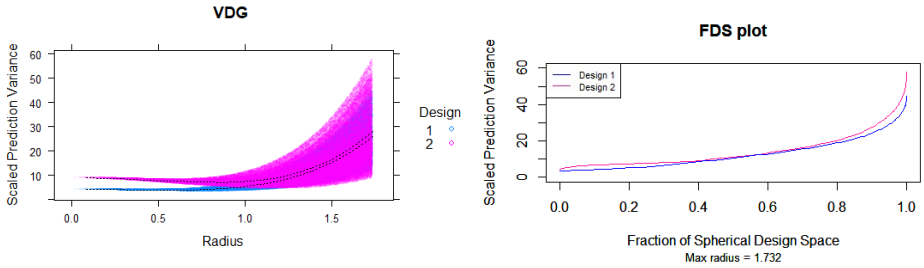

Figure 4.1: VDG and FDS plot for 24-run Bayesian I-optimal design (1) and Bayesian D-optimal design (2)

D-optimal designs. From the VDG, we can observe that Bayesian D-optimal design has higher average SPV values than Bayesian I-optimal design throughout the whole design region. Given a radius, the maximum SPV of Bayesian I-optimal design is always smaller than that of Bayesian D-optimal design. From the FDS plot we observe that Bayesian I-optimal design has relatively flatter curve uniformly thorughout the whole design region, indicating that Bayesian I-optimal design have comparatively less fluctuating SPV values than Bayesian D-optimal design for the whole design region. For a possible SPV value, Bayesian D-optimal design has a smaller fraction of design space than

Bayesian I-optimal design, for which the SPV values are less than or equal to the given SPV value.

Figure 4.2 shows the boxplots of the SPV values for Bayesian I-optimal

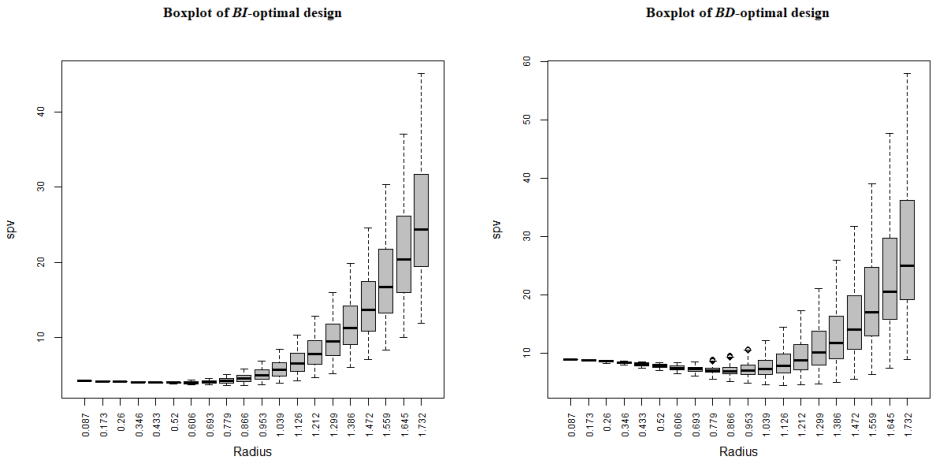

Figure 4.2: Boxplots for 24-run Bayesian I-optimal design and Bayesian D-optimal design

(BI-optimal) design and Bayesian D-optimal (BD-optimal) design with respect to various radii starting from 0.087 to 1.732. The boxplots indicate that, for all radii, the Bayesian D-optimal design has longer whisker on the upper side than Bayesian I-optimal design conforming that Bayesian I-optimal design is more symmetric than Bayesian D-optimal design in terms of SPV values.

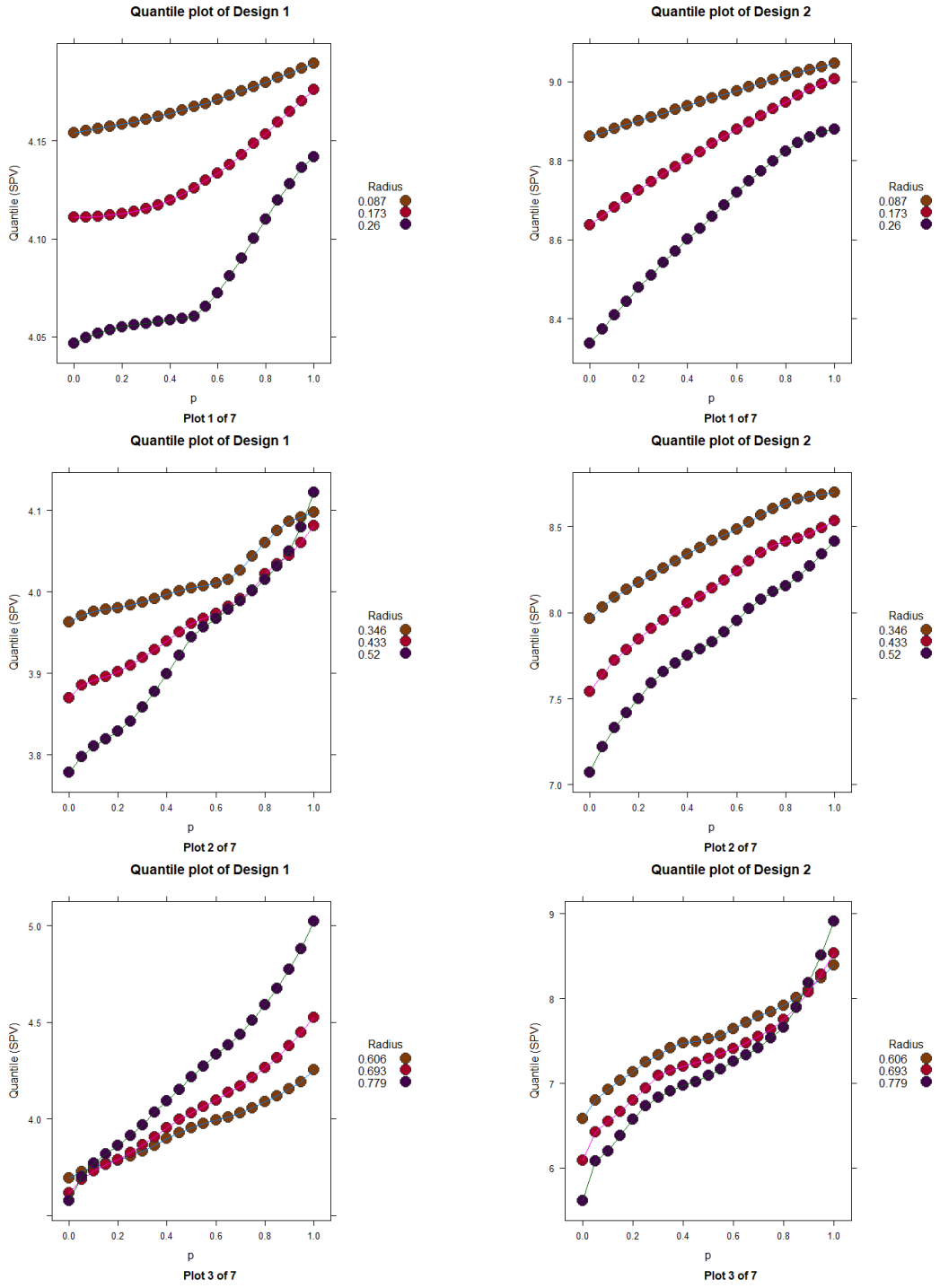

Figure 4.3: Quantile plots (plots 1 to 3) for 24-run Bayesian I-optimal design (1) and Bayesian D-optimal design (2)

Figure 4.3, 4.4 and 4.5 provide the quantile plots for both Bayesian I- and Bayesian D-optimal designs at 20 specific gradually increasing radii. It can be observed from plot 1 that when the radius is approximately equal to 0.087, the designs are nearly rotatable as the SPV values does not vary much over the hypersphere. Although, both designs are rotatable at the smallest radius, the SPV values are lower for Bayesian I-optimal design (approximately from 4.15 to 5.0) than Bayesian D-optimal design, which are greater than or equal to 8.9. As the radii increase (depicted in plot 2 to plot 7) the ecdf's for both the designs become steeper and the designs tend to be less rotatable.

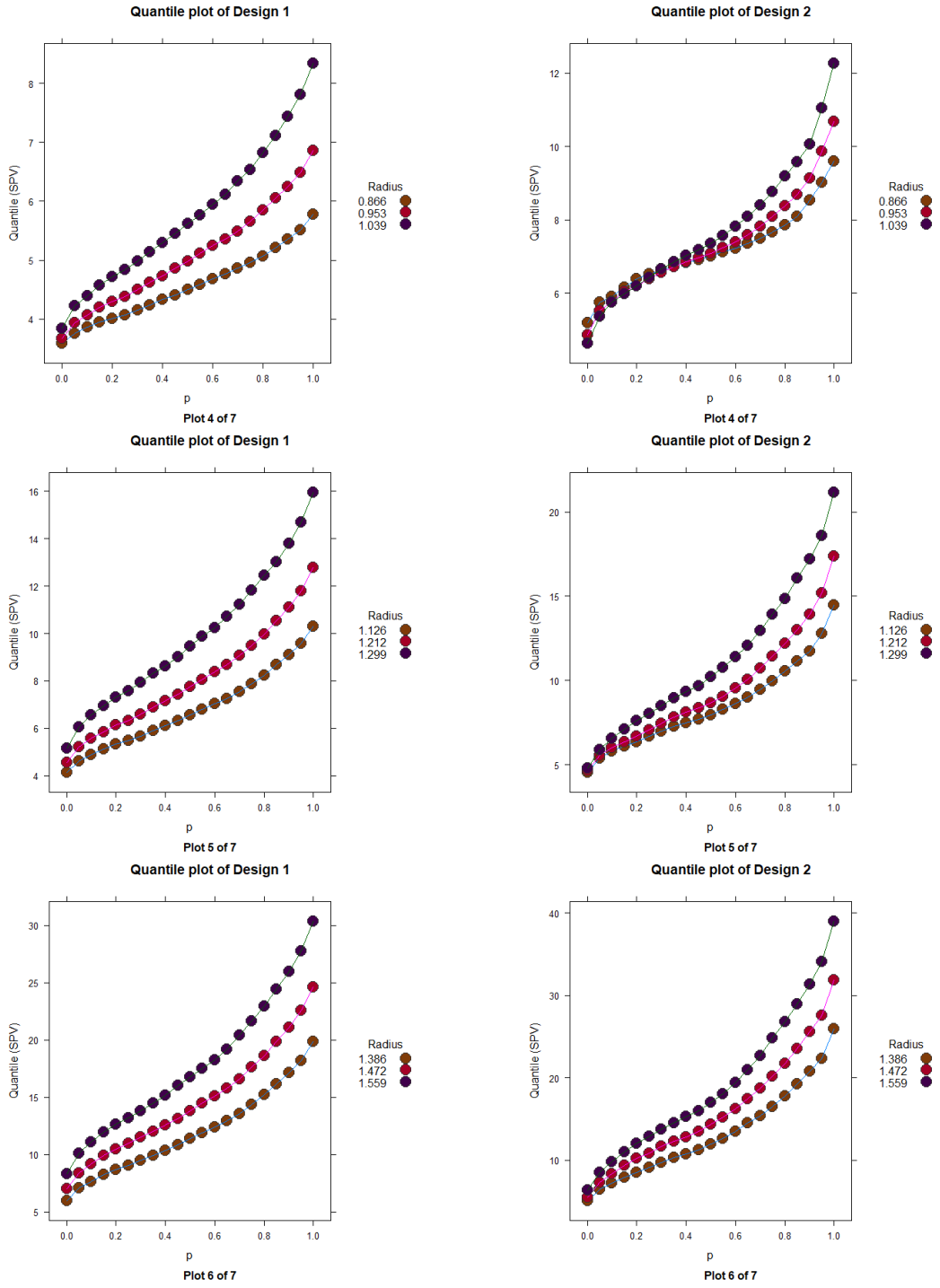

Figure 4.4: Quantile plots (plots 4 to 6) for 24-run Bayesian I-optimal design (1) and Bayesian D-optimal design (2)

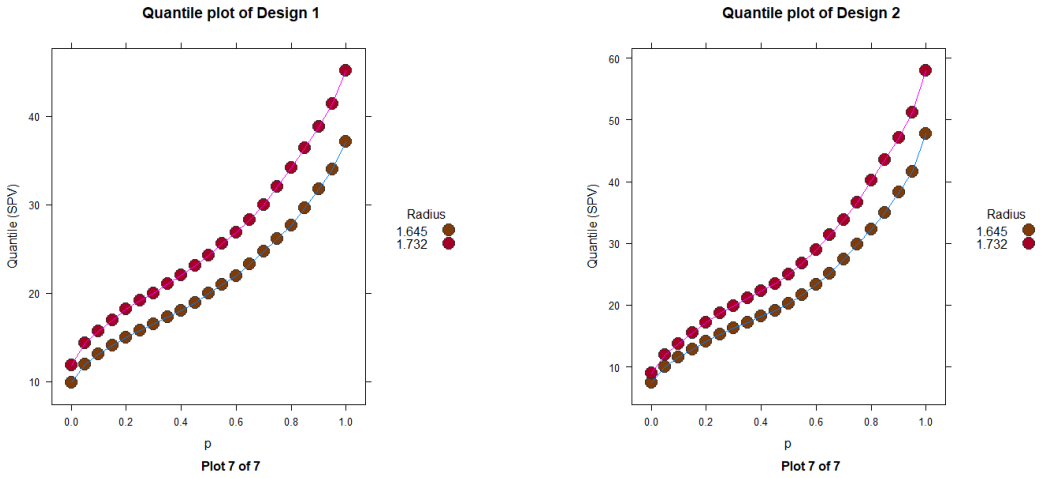

Figure 4.5: Quantile plot (plot 7) for 24-run Bayesian I-optimal design (1) and Bayesian D-optimal design (2)

Figure 4.6 contains the combined quantile plots for each radii and indicates that Bayesian I-optimal design outperforms Bayesian D-optimal design at each radius in terms of lower prediction variance of the response, even though for larger radii, the difference is nominal.

Overall, we can conclude that Bayesian D-optimal design has higher SPV values than Bayesian I-optimal design throughout the whole experimental region and from the FDS plot we can conclude that Bayesian I- optimal design has relatively flatter curve uniformly thorughout the whole design space, indicating that Bayesian I-optimal design have comparatively less fluctuating SPV values than Bayesian D-optimal design for the whole design space. In general, Bayesian I-optimal design has a better prediction capability in the whole design space.

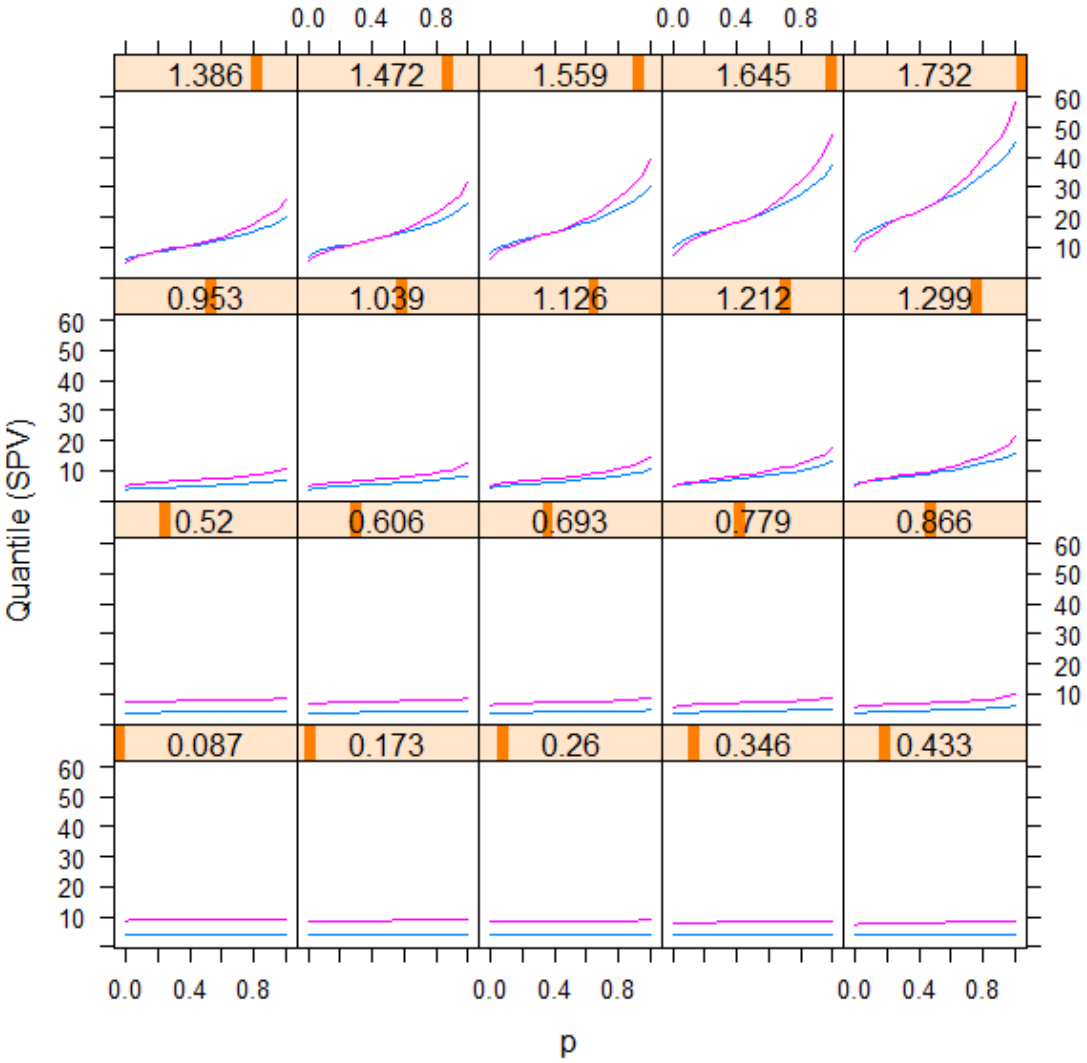

Figure 4.6: Quantile plots for 24-run Bayesian I-optimal design (Blue) and Bayesian D-optimal design (Pink)

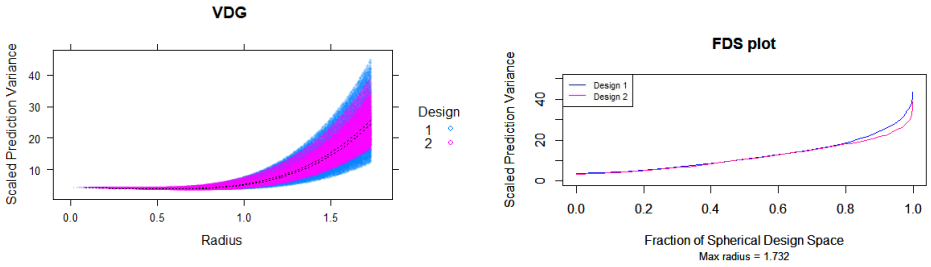

Figure 4.7: VDG and FDS plot for 24-run Bayesian I-optimal design (1) and Bayesian IP-optimal design (2)

Figure 4.7 provides the VDG and FDS plot of Bayesian I- and Bayesian IP- optimal design. When compared on the basis of Bayesian I-optimality criterion, the Bayesian IP-optimal design performs better than the Bayesian I-optimal design as it has smaller range of SPV values and more stable FDS plot in the design region than that of Bayesian I-optimal design.

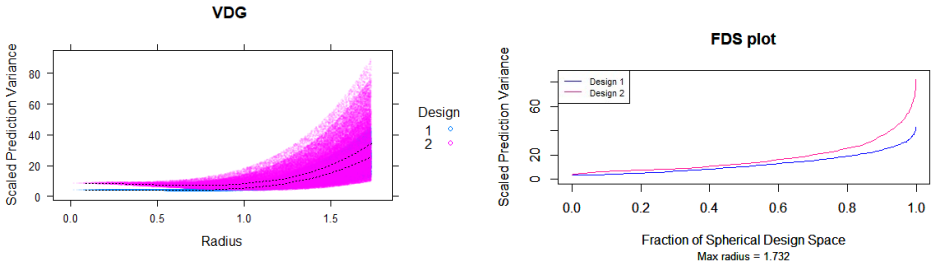

Figure 4.8: VDG and FDS plot for 24-run Bayesian I-optimal design (1) and Bayesian DP-optimal design (2)

Figure 4.8 shows the VDG and FDS plot of Bayesian I- and Bayesian DP-optimal design, which reveals that the latter has a wider range of SPV values and a steeper FDS plot than the former. Hence, it can be concluded that Bayesian I-optimal design has a better prediction property than Bayesian

DP-optimal design over the whole design region.

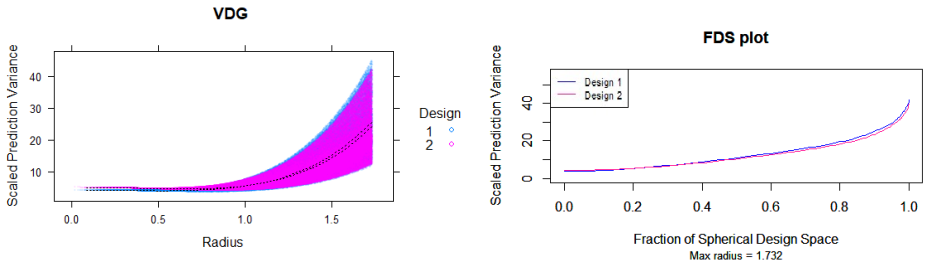

Figure 4.9: VDG and FDS plot for 24-run Bayesian I-optimal design (1) and Bayesian I_D-optimal design (2)

From the VDG and FDS plot of Bayesian I- and Bayesian I_D-optimal designs in Figure 4.9, we notice that Bayesian I_D-optimal design is slightly superior than Bayesian I-optimal design uniformly throughout the entire design region.

Figure 4.10 presents the VDG and FDS plot for Bayesian I- and Bayesian

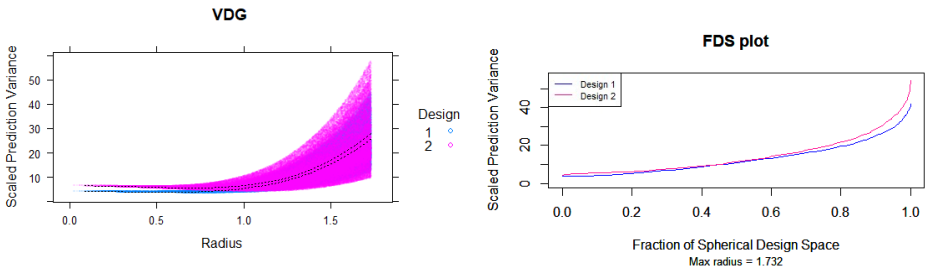

Figure 4.10: VDG and FDS plot for 24-run Bayesian I-optimal design (1) and Bayesian I_DP-optimal design (2)

I_DP-optimal designs. We can distinguish that Bayesian I-optimal design is slightly superior than Bayesian I_DP-optimal design uniformly throughout the entire design region, notably near the perimeter of the experimental region.

Although the FDS plot shows that both the designs have similar pattern of fluctuation for smaller SPV values up to approximately 70% of the design space, overall it can be deduced that Bayesian I_DP- optimal design performs similarly but less efficiently than Bayesian I-optimal design.

Figure 4.11 represents the VDGs for Bayesian I-, Bayesian IP-, Bayesian

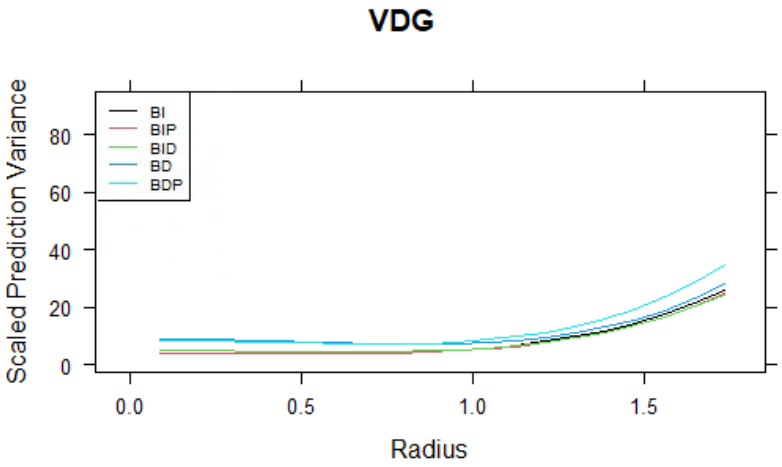

Figure 4.11: VDGs for 24-Run Bayesian optimal designs

I_D-, Bayesian D- and Bayesian DP-optimal designs. Each curve represents the average SPV of the a designs. For an enhanced depiction Bayesian I_DP is not considered in the overall comparison, owing to it's excessively large SPV values. From Figure 4.11 we can observe that, overall, with increasing radii the curves get steeper and for smaller radii (from the origin up to radii 1.0) the average SPV values are relatively stable for all the Bayesian optimal designs. However, the average SPV values for Bayesian D- and Bayesian DP-optimal designs

start off at a relatively higher position than that of Bayesian I-, Bayesian IP- and Bayesian I_D-optimal designs.

Based on the VDGs in Figure 4.11, it is difficult to distinguish which design performs significantly better among Bayesian I-, Bayesian IP- and Bayesian I_D-optimal designs. Therefore, we used the combined FDS plots and variance ratio FDS plot for further distinction.

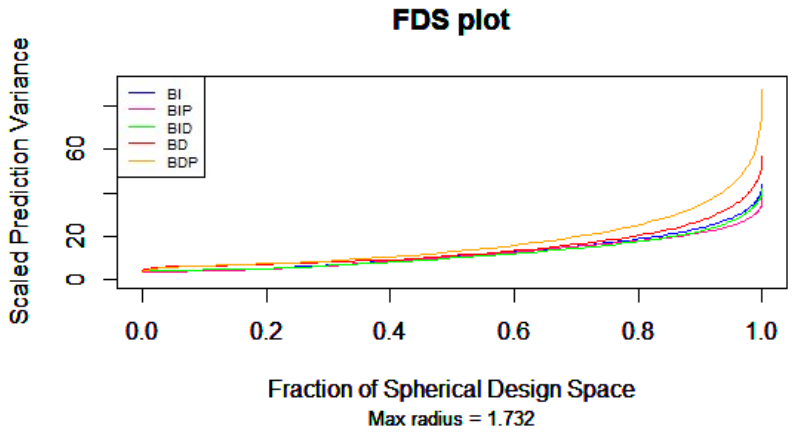

Figure 4.12: FDS plots for 24-run Bayesian Optimal designs

Figure 4.12 provides combined FDS plots for the Bayesian optimal designs. From the plots, we can come to the conclusions that corroborate with the ones obtained from VDGs. Bayesian D- and Bayesian DP-optimal designs have relatively stable SPV values for 50% of the total design space, while for the Bayesian I-, Bayesian IP- and Bayesian I_D- optimal designs, lesser fluctuation in SPV values is observed in about 70% of the total design space. In 10% of the design space where the highest SPV values occur, Bayesian IP-optimal

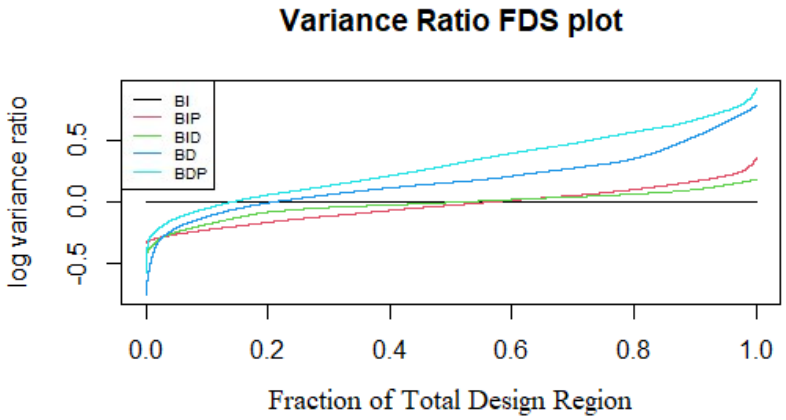

Figure 4.13: Variance Ratio FDS plots for 24-run Bayesian optimal designs

design turns out to be better than both Bayesian I- and Bayesian I_D-optimal designs.

Figure 4.13 is the variance ratio FDS plot for Bayesian optimal designs with Bayesian I-optimal design as the reference design. Since the reference design has a constant variance ratio, it is characterized by the black horizontal line in the plot. When we minutely observe Figure 4.13, we can identify that although the curve for Bayesian I_D-optimal design seems to be flatter than Bayesian IP-optimal design, the curve of the latter design is below the black horizontal line for approximately 60% of the total design space. When Bayesian I-optimal design is the reference design, the variance ratio for of Bayesian IP-optimal design is less than one for relatively most part of the design space, and is therefore preferable as it leads to better predictions over most of the experimental region.

Finally, based on the graphs in Figure 4.11 and Figure 4.12 we can conclude that, when compared on the basis of prediction abilities, Bayesian IP-optimal design performs better than Bayesian I-optimal design. Therefore, when prime interest is to make predictions about future observations, Bayesian IP-optimal design is capable of yielding more precise prediction in comparison to other Bayesian optimal designs.

4.2 30-Run 4-Factor Bayesian Optimal Designs

In this section, we compare 30-run 4-factor Bayesian optimal designs with the 30-run 4-factor Bayesian I-optimal design. Figure 4.14 contains the VDG and

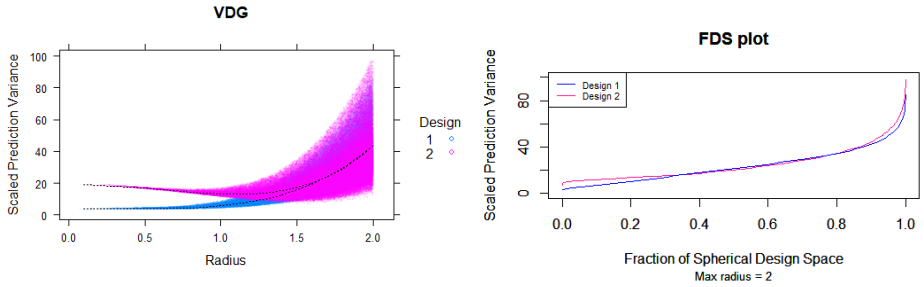

Figure 4.14: VDG and FDS plot for 30-run Bayesian I-optimal design (1) and Bayesian D-optimal design (2)

FDS plot for Bayesian I- and Bayesian D-optimal designs. The VDG indicates that the average SPV values of the Bayesian D-optimal design are higher than that of Bayesian I-optimal design when the radius is less than 1.5. However, after radius 1.5, the average SPV curves of both designs overlap. Note that,

majority of the SPV values occur at the peripheral area of the deisgn space, after radius 1.0. From the FDS plot we can interpret that both designs have the same pattern of fluctuation in the SPV values, within the range of 20 to 40, for approximately more than 50% of the design space. Nevertheless, the Bayesian I-optimal design has less fluctuating SPV values in the entire region than Bayesian D-optimal design, being more preferable.

Figure 4.15 provides the VDG and FDS plot of Bayesian I- and Bayesian

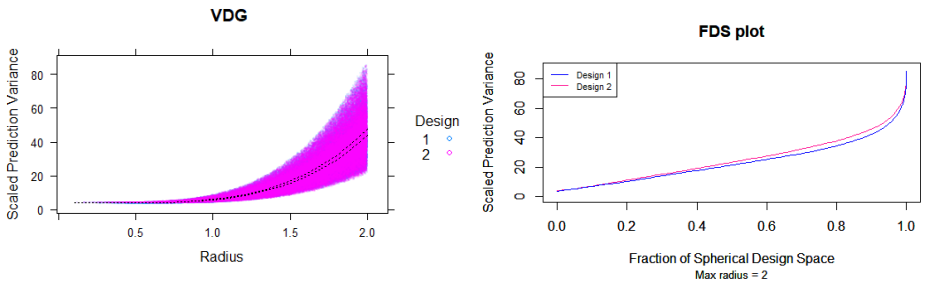

Figure 4.15: VDG and FDS plot for 30-run Bayesian I-optimal design (1) and Bayesian IP-optimal design (2)

IP-optimal design. It appears from the VDG and FDS plot of the two designs that the average SPV curve and FDS curve of Bayesian I-optimal design are at a slightly lower position than that of Bayesian IP-optimal design. In order to examine exhaustively and to identify if there is any significant difference between the two designs, we constructed boxplots and quantile plots for Bayesian I- and Bayesian IP-optimal design.

Figure 4.16 shows the boxplots of the SPV values for Bayesian I-optimal (BI-optimal) design and Bayesian IP-optimal (BIP-optimal) design with re-

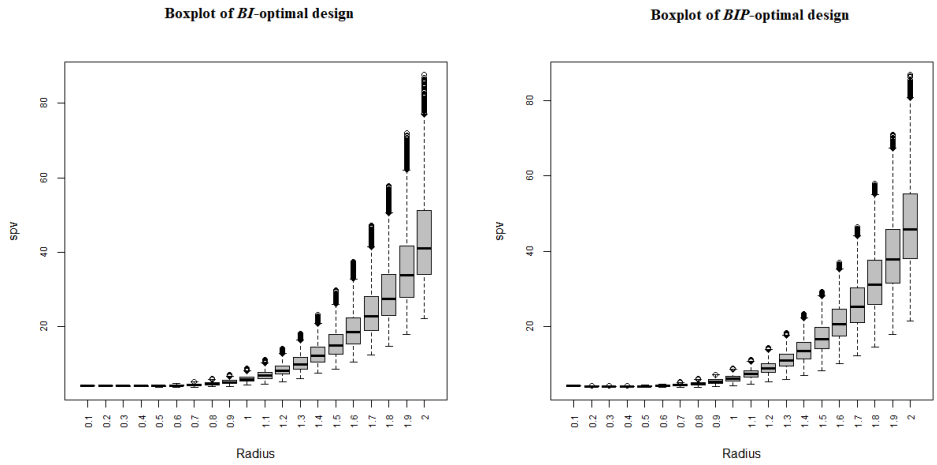

Figure 4.16: Boxplots for 30-run Bayesian I-optimal design and Bayesian IP-optimal design

spect to 20 radii, with minimum value at 0.1 up to maximum radius at 2. The boxplots reveal that the SPV distributions of the designs are approximately symmetric for a given radius, although the SPV values of Bayesian IP-optimal design apprears to be more symmetric than that of Bayesian I-optimal design. With increasing radii, the former design has more frequency of higher SPV values near the design perimeter than the latter.

Figure 4.17, Figure 4.18 and Figure 4.19 provide the quantile plots for both Bayesian I- and Bayesian D-optimal designs at 20 specific gradually increasing radii. The quantile plots depict that, the Bayesian I-optimal design is not rotatable at any point of the design space as the SPV values are not stable and persistently increases over the entire design region. On the other hand, the Bayesian IP-optimal design is nearly rotatable at ra-

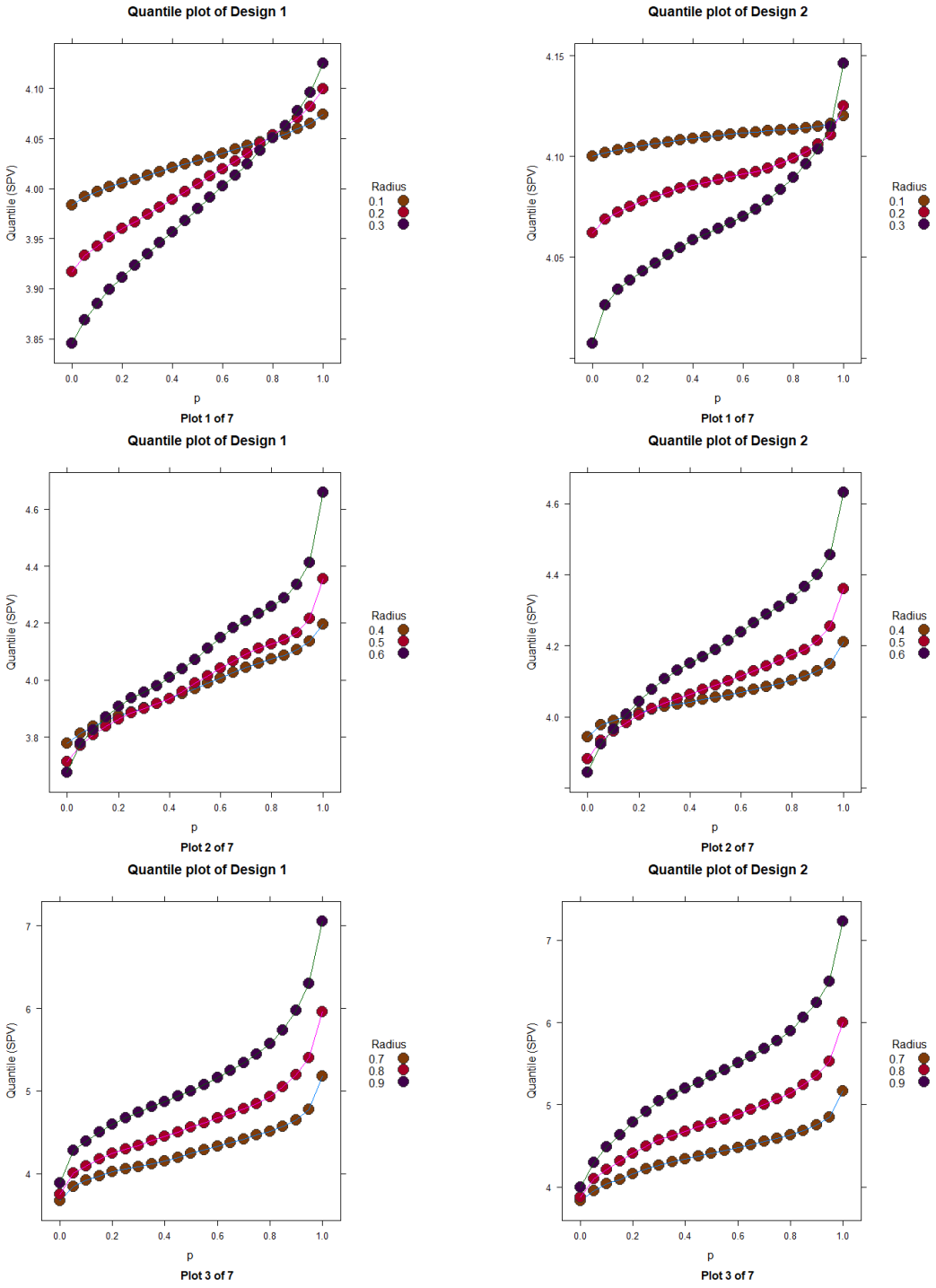

Figure 4.17: Quantile plots (plots 1 to 3) for 30-run Bayesian I-optimal design (1) and Bayesian IP-optimal design (2)

dius 0.1 with SPV value at approximately 4.10. However, the pattern of the SPV values at all subsequent radii (plot 2 to plot 7) are similar for both designs.

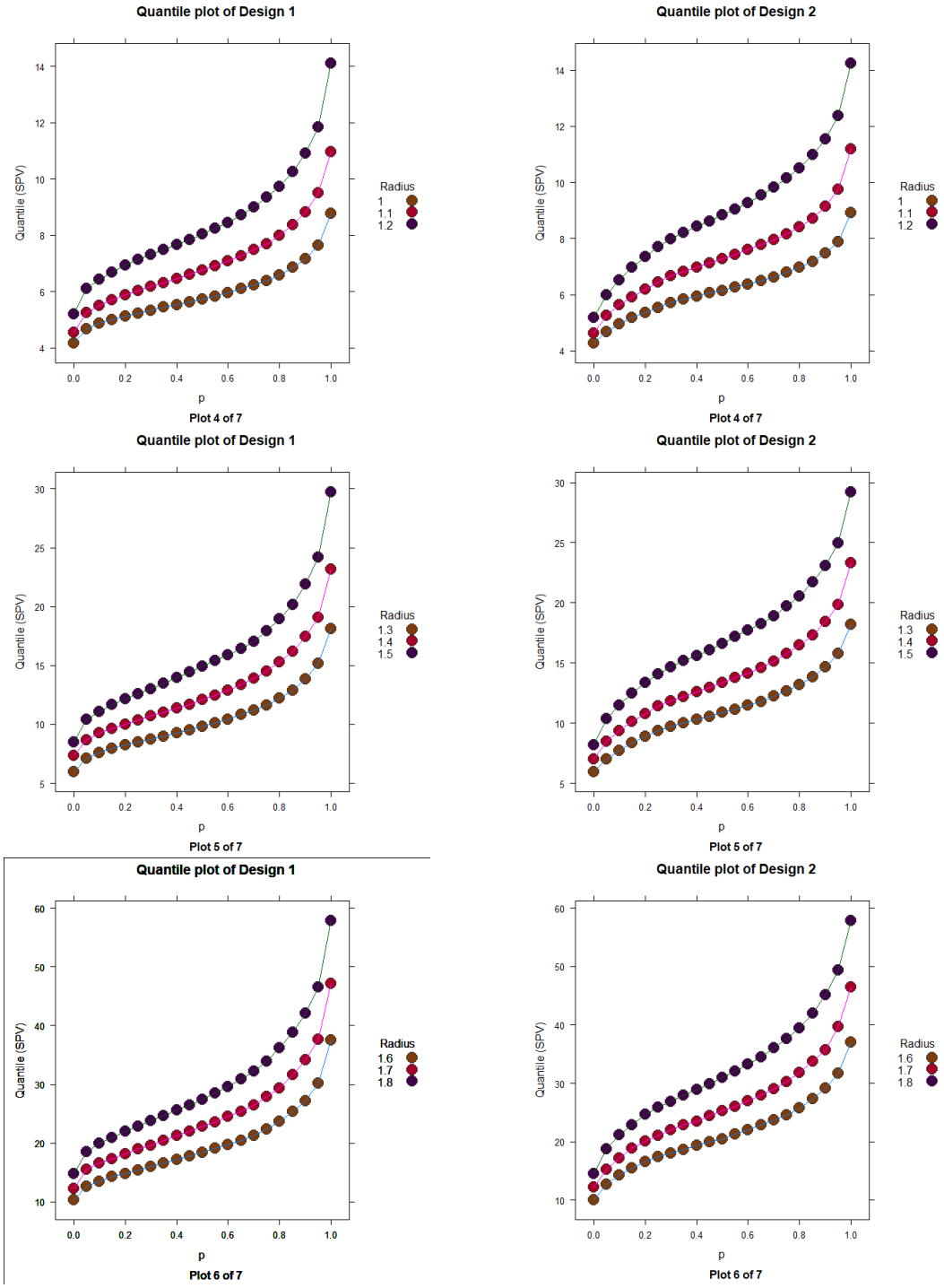

Figure 4.18: Quantile plots (plots 4 to 6) for 30-run Bayesian I-optimal design (1) and Bayesian IP-optimal design (2)

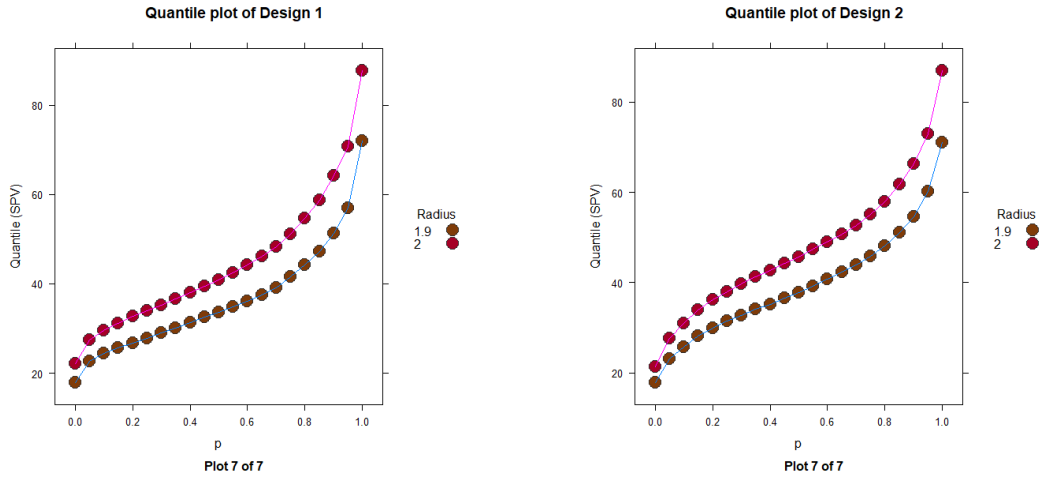

Figure 4.19: Quantile plot (plot 7) for 30-run Bayesian I-optimal design (1) and Bayesian IP-optimal design (2)

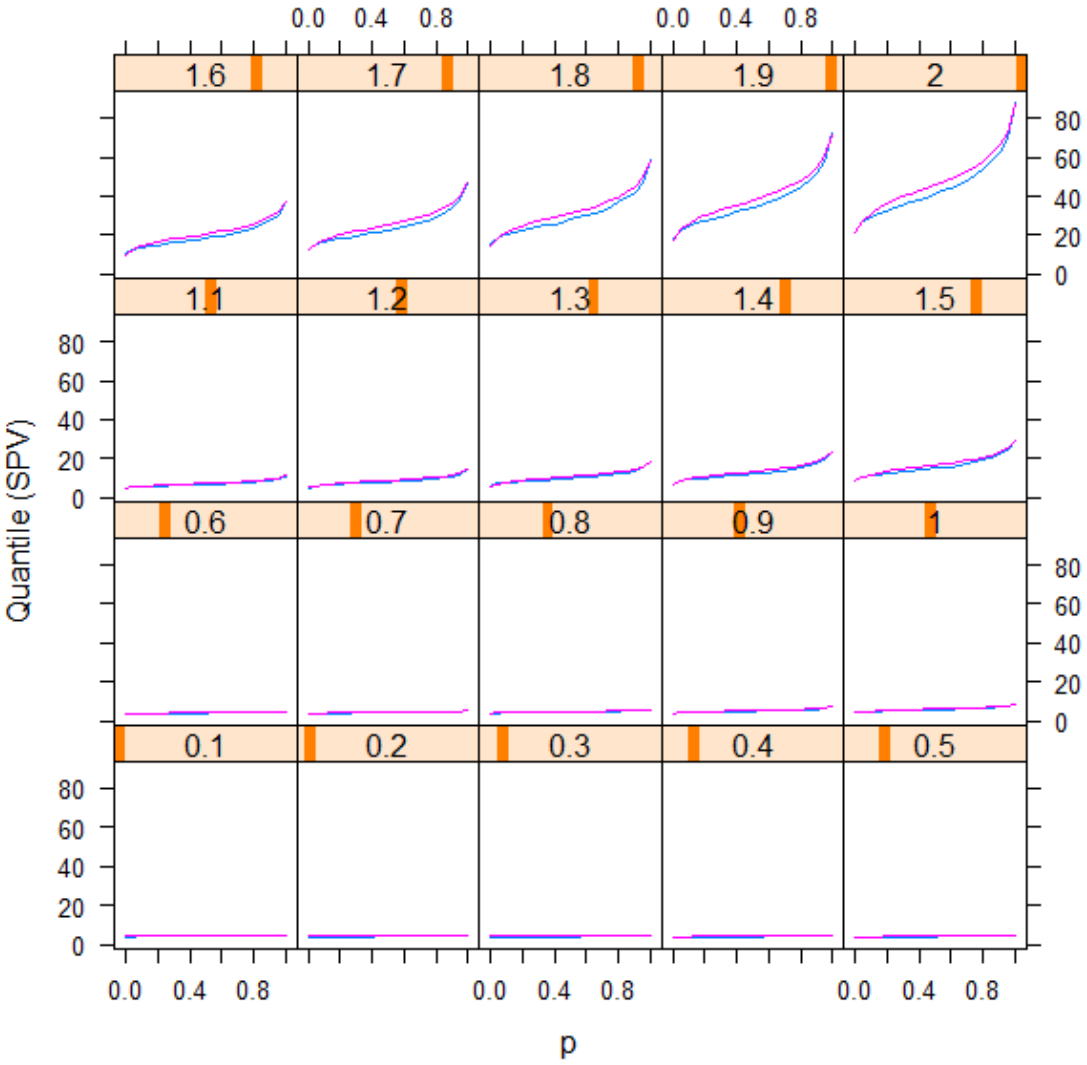

Figure 4.20: Quantile plots for 30-run Bayesian I-optimal design (Blue) and Bayesian IP-optimal design (Pink)

Figure 4.20 provides the quantile plots for both designs at 20 different radii in a different way. For each radius, the quantile plots for both designs are

in the same plot, so that we can see the difference clearly. We can conclude from Figure 4.20 that, there is no significant difference in the SPV values of Bayesian I- and Baysian IP-optimal design up to radius 1.4. Bayesian I-optimal design emerges to be slightly better with comparatively lower SPV values than Bayesian IP-optimal design when radius is 1.5 and above.

Figure 4.21 shows the VDG and FDS plot of Bayesian I- and Bayesian

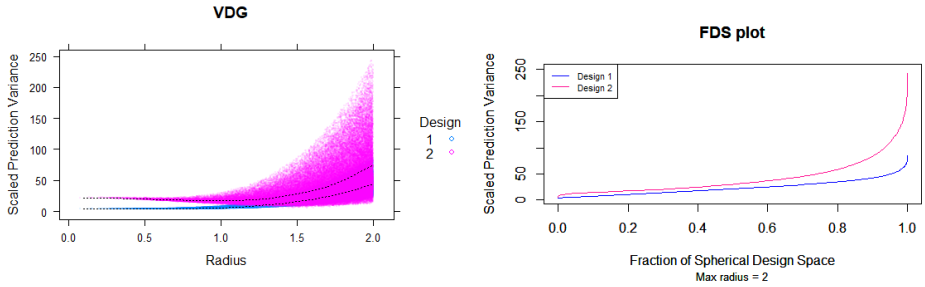

Figure 4.21: VDG and FDS plot for 30-run Bayesian I-optimal design (1) and Bayesian DP-optimal design (2)

DP-optimal designs. Based on the graphs it is evident that the latter design performs poorly in terms of prediction abilities than the former. The VDG show that the both maximum and average SPV curve of Bayesian DP-optimal design are at a distinctly higher level than that of Bayesian I-optimal design. From the FDS plot we can see that at the SPV value 50, the corresponding values in the x-axis are approximately 0.95 and 0.70 for Bayesian I- and Bayesian DP-optimal designs, respectively. These values imply that, 95% of the entire design space of Bayesian I-optimal design has SPV value less than or equal to 50, whereas the corresponding fraction for the Bayesian DP-optimal design

is around 70%. Overall, the Bayesian I-optimal design performs significantly better in terms of prediction capability than the Bayesian DP-optimal design.

From the VDG and FDS plot of Bayesian I- and Bayesian I_D-optimal

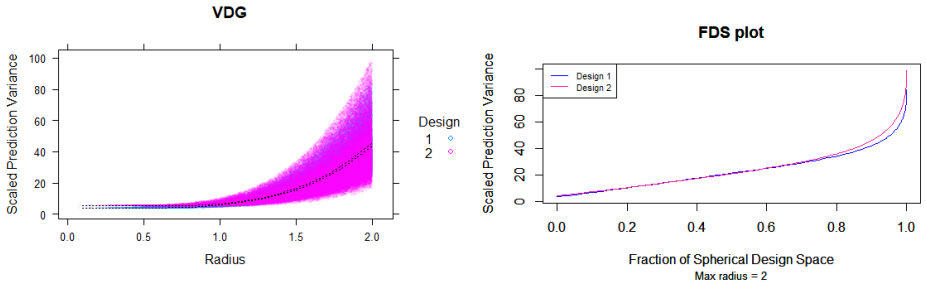

Figure 4.22: VDG and FDS plot for 30-run Bayesian I-optimal design (1) and Bayesian I_D-optimal design (2)

designs in Figure 4.22, we can observe that both the designs have similar distribution of SPV values over most of the design space. The average SPV curve in the VDG of both designs are almost superimposed on each other. The FDS plots reveal that for up to 80% of the entire the design space when the SPV values are less than 40, both designs have exactly same pattern of fluctuating SPV values. Bayesian I-optimal design turns out to be slightly superior in the remaining 20% of the design space where the SPV values are more than 45.

Figure 4.23 presents the VDG and FDS plot for Bayesian I- and Bayesian I_DP-optimal designs. The VDG show that the average SPV curves of both designs are almost conjoining up to radius 1.5. We can observe from the FDS plot that both designs perform almost similarly for 50% of the entire design

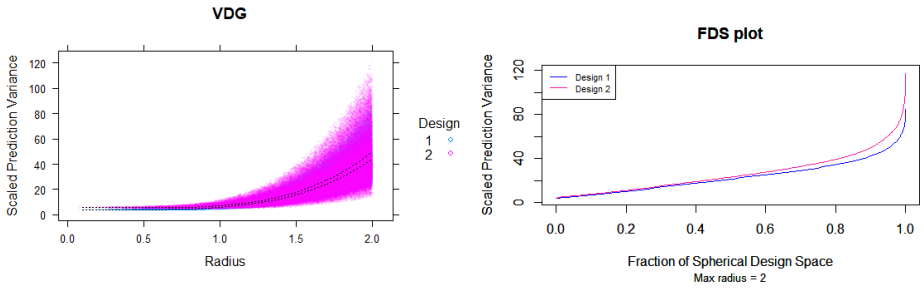

Figure 4.23: VDG and FDS plot for 30-run Bayesian I-optimal design (1) and Bayesian I_DP-optimal design (2)

space when the SPV values are below 23. With the increasing SPV values, the difference between the two designs appears to be prominent and Bayesian I-optimal design emerges to be better than Bayesian I_DP-optimal design.

Figure 4.24 provides the VDGs for Bayesian I-, Bayesian D-, Bayesian

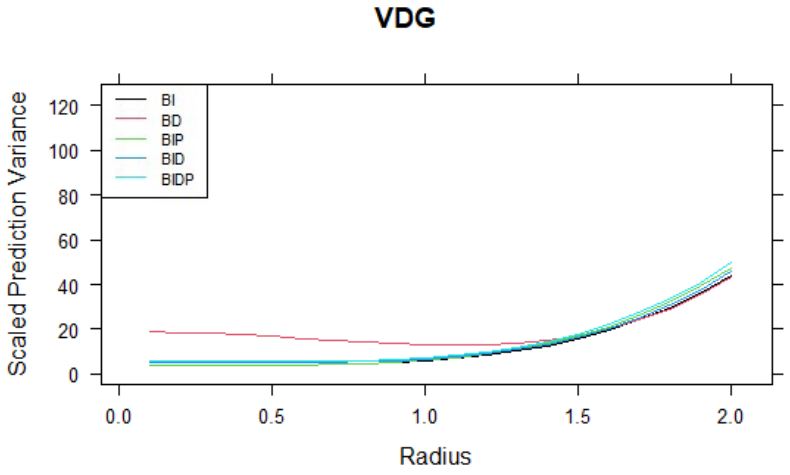

Figure 4.24: VDGs for 30-run Bayesian Optimal Designs

IP-, Bayesian I_D- and Bayesian I_DP-optimal designs. As the SPV values of

Bayesian DP-optimal design are excessively large, it is not considered in the overall comparison. From Figure 4.24 we can observe that overall, except for Bayesian D-optimal design, the average SPV values of all other Bayesian optimal designs start with relatively smaller values near the origin, and consistently increase with increasing radii. Although, the average SPV values for Bayesian D-optimal designs start off at a relatively higher position than the reamining designs, after radius 1.5, the average SPV curves of all the designs are hardly distinguishable. Hence, for better illustration, we focused on the combined FDS plots and variance ratio FDS plot.

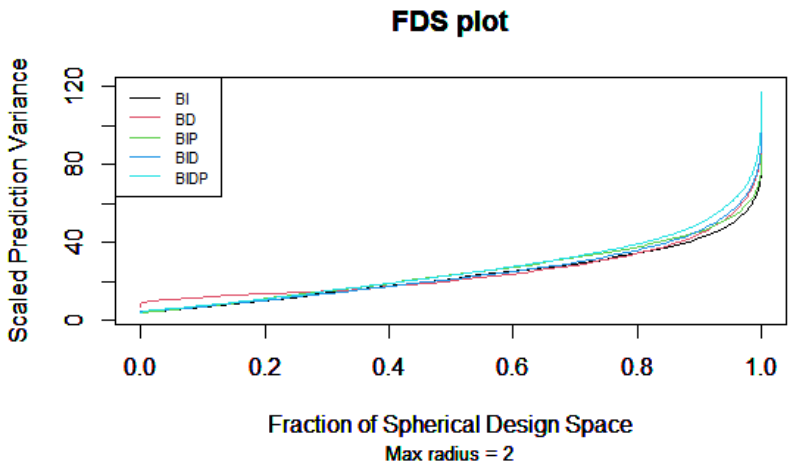

Figure 4.25: FDS plots for 30-run Bayesian Optimal Designs

Figure 4.25 and Figure 4.26 provide combined FDS plots and Variance ratio FDS plot for the Bayeisan optimal designs, respectively. From the combined FDS plots, we can observe that all the Bayesian optimal designs have

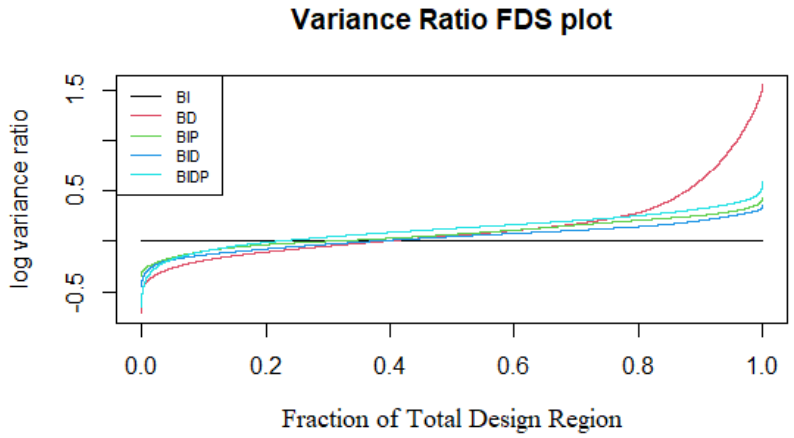

Figure 4.26: Variance Ratio FDS plots for 30-run Bayesian Optimal designs

comparatively less digressing SPV for approximately 75% of the total experimental region, when the SPV vaules are less than 30. In the remaining 25% of the entire region, where high SPV values occur, Bayesian I_DP-optimal design perfroms poorly having relatively higher prediction variance (with highest SPV value at 117.5) in comparison to other Bayesian optimal designs.

In Figure 4.26, as the differences between the designs are magnified using the log variance ratio, it becomes evident that Bayesian IP-, Bayesian I_D- and Bayesian I_DP-optimal designs perform almost similarly when compared with the reference Bayesian I-optimal design as the log variance ratios for these designs are less than one. Only design with log variance ratio more than one is the Bayesian D-optimal design, indicating it predicts worse than the reference design.

Overall, we can infer that when predictions are required near the origin, Bayesian I-, Bayesian IP- and Bayesian I_D-optimal design can be alternative choices. On the other hand, if the predictions are required at the perimeter, then Bayesian I-optimal design is the ultimate choice.

Chapter 5

Comparison of Bayesian Optimal Designs with I-Optimal Design

This chapter presents a comparative illustrations of Bayesian optimal designs with I-optimal design. Thus, for comparison purpose, the scaled prediction variance and the average prediction variance are calculated by the formulas (2.7) and (2.11), respectively. The model consists of the main and quadratic effects only.

In section 5.1, we compare 24-run 3-factor Bayesian optimal designs with the I-optimal design in Table 2.1. In section 5.2, we compare 30-run 4-factor Bayesian optimal designs with the I-optimal design in Table A.3 in Appendix. For overall comparison in both sections, we have constructed combined VDG, FDS plot and variance ratio FDS plot.

5.1 24-Run 3-Factor Bayesian Optimal Designs

In this section, we will compare the 24-run 3-factor Bayesian optimal designs with the 24-run 3-factor I-optimal design in Table 2.1. Figure 5.1 provides

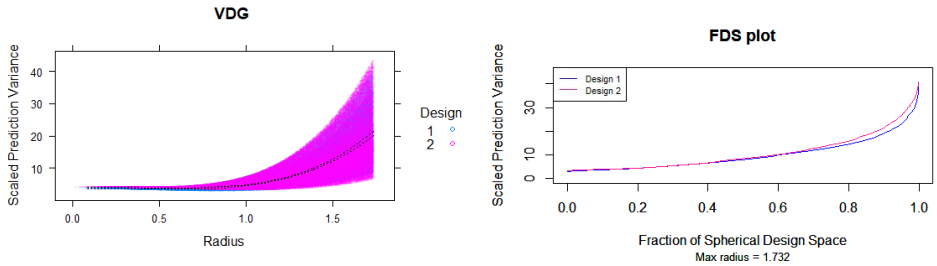

Figure 5.1: VDG and FDS plot for 24-run I-optimal design (1) and Bayesian I-optimal design (2)

the VDG and FDS plot for I-optimal and Bayesian I-optimal designs. From the VDG, we see that the spread of SPV values for both designs are similar, with Bayesian I-optimal design having slightly higher average SPV values than I-optimal design near the perimeter of the design region. The FDS plot depict that the Bayesian I-optimal design performs almost analogously with I-optimal design, up to 65% of the whole design space. Notably, for 30% of the total design space where relatively higher SPV values occur, the Bayesian I-optimal design tends to have the FDS curve at an upper level than I-optimal design.

Figure 5.2 shows the VDG and FDS plot for I- and Bayesian D-optimal design. The VDG reveal that, the distribution of SPV for Bayesian D-optimal design start off at a relatively higher point than that of I-optimal design. The average SPV curve of Bayesian D-optimal design is persistently higher than

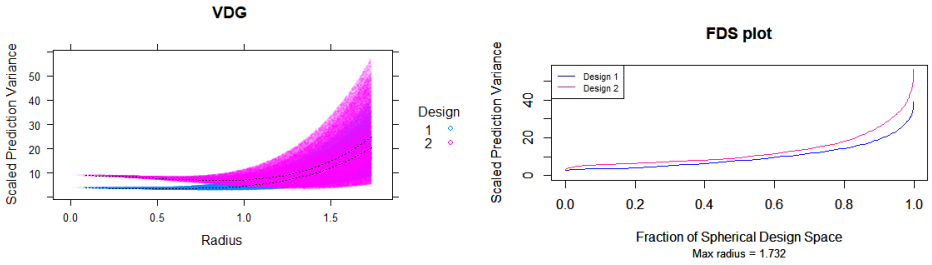

Figure 5.2: VDG and FDS plot for 24-run I-optimal design (1) and Bayesian D-optimal design (2)

I-optimal design. From the FDS plot, we can observe that Bayesian D-optimal design has higher and more fluctuating SPV values than the I-optimal design consistantly thoroughout the entire design space.

Figure 5.3 displays the VDG and FDS plot for I- and Bayesian IP-

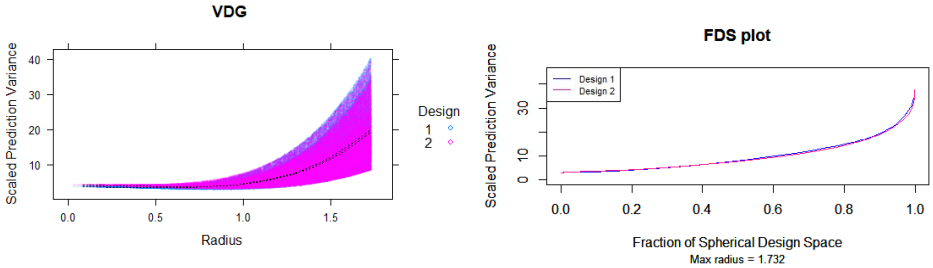

Figure 5.3: VDG and FDS plot for 24-run I-optimal design (1) and Bayesian IP-optimal design (2)

optimal design. From the VDG, we can notice that the spread of SPV values of both designs are alike. The minimum SPV curve for both designs align with each other. However, the maximum and average SPV curves of Bayesian IP-optimal design are relatively lower than I-optimal design near the perimeter of the design region. The FDS plot depicts that Bayesian IP-optimal design

emerges to be slightly better than the I-optimal design as it can be seen the SPV values for the former design is comparatively smaller and more stable than that of the latter one.

Figure 5.4 provides the VDG and FDS plot for I- and Bayesian DP-

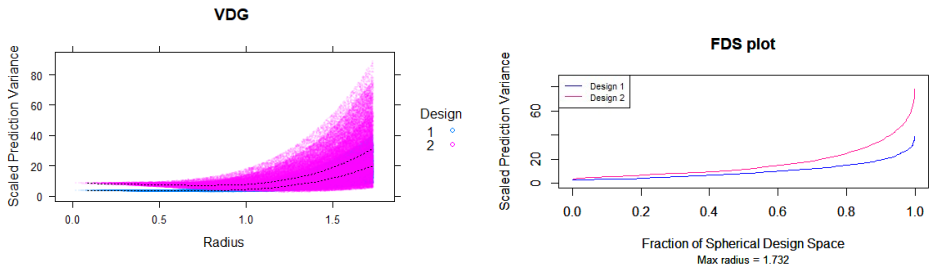

Figure 5.4: VDG and FDS plot for 24-run I-optimal design (1) and Bayesian DP-optimal design (2)

optimal design. The graphs indicate that Bayesian DP-optimal design has a wider range of SPV values in comparison to I-optimal design. With minor difference in the minimum SPV curves of both designs, the VDG show that the maximum and average SPV curves of Bayesian DP-optimal design are at significantly higher level than that of I-optimal design. The FDS plot is flatter for the I-optimal design than Bayesian DP-optimal design, with the difference becoming prominent in 50% of the total design space with relatively higher SPV values.

Figure 5.5 shows the VDG and FDS plot for I- and Bayesian I_D-optimal design. The VDG of both designs reflect that there are no remarkable differences between the minimum, maximum and average SPV curves of respective

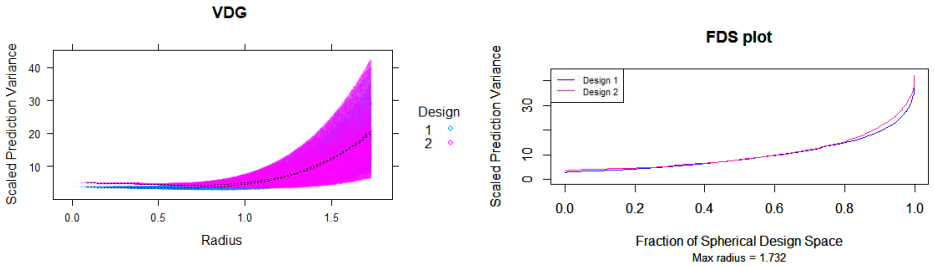

Figure 5.5: VDG and FDS plot for 24-run I-optimal design (1) and Bayesian I_D-optimal design (2)

designs. The graphs reveal that Bayesian I_D-optimal design seems to perform equally well as the I-optimal design, in terms of smaller and stable SPV values in 80% of the total design space. However, in the remaining 20% of the total design space when higher SPV values occur, the I-optimal design is slightly superior.

Figure 5.6 provides the VDG and FDS plot for I- and Bayesian I_DP-

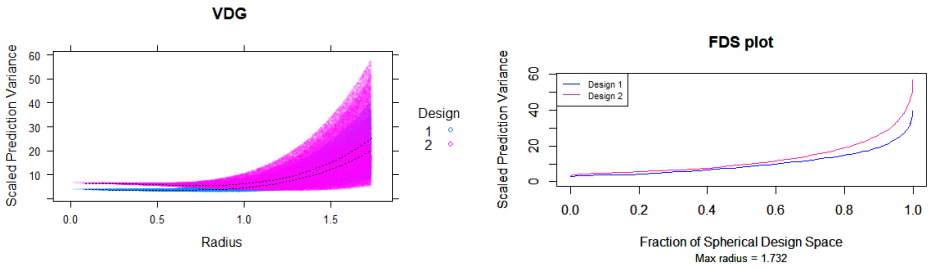

Figure 5.6: VDG and FDS plot for 24-run I-optimal design (1) and Bayesian I_DP-optimal design (2)

optimal design. The latter design seems to have higher SPV values than that of the former design throughout the entire experimental region. The VDG portray that, maximum SPV curve of Bayesian I_DP-optimal design is distinctly higher

than that of I-optimal design throughout the entire design region. Although, the deviation between the average SPV curves of the two designs is less eminent. On the other hand, the FDS plot reveals that for 50% of the total design space, both the designs have similar pattern of fluctuation in the SPV values, the difference becomes noteworthy in the remaining 50%, when the SPV values are greater than 10.

Figure 5.7 presents the VDG for Bayesian I-, Bayesian IP-, Bayesian

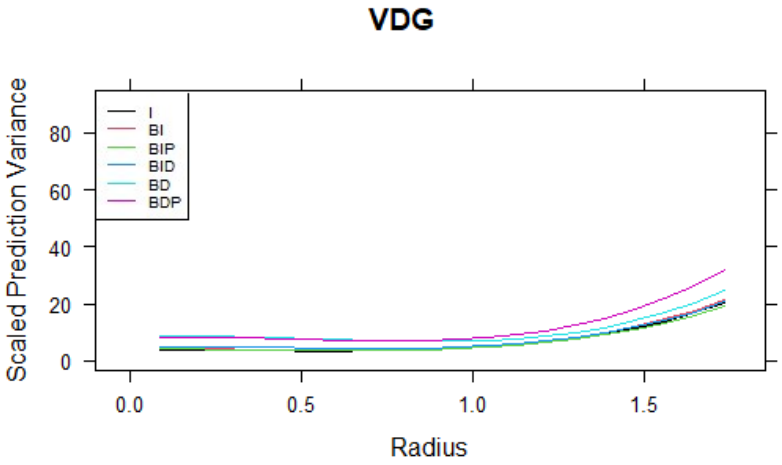

Figure 5.7: VDG for 24-run I-optimal design and Bayesian dptimal designs

I_D-, Bayesian D-, Bayesian DP- and I-optimal design. Each curve indicates the average SPV of the designs. For a magnified illustration, Bayesian I_DP is not considered in the overall comparison, owing to it's excessively large SPV values.

From Figure 5.7 we observe that, overall, the average SPV values are

less than 40 for all the Bayesian optimal designs including the I-optimal design. The average SPV values for Bayesian D- and Bayesian DP-optimal designs start off at a relatively higher position than other designs. While on the other hand, the average SPV curves of the I-, Bayesian I-, Bayesian IP- and Bayesian I_D-optimal designs are almost overlapping. In this situation, for better distinction, we used the combined FDS plots and variance ratio FDS plot.

Figure 5.8 and Figure 5.9 include combined FDS plot and variance

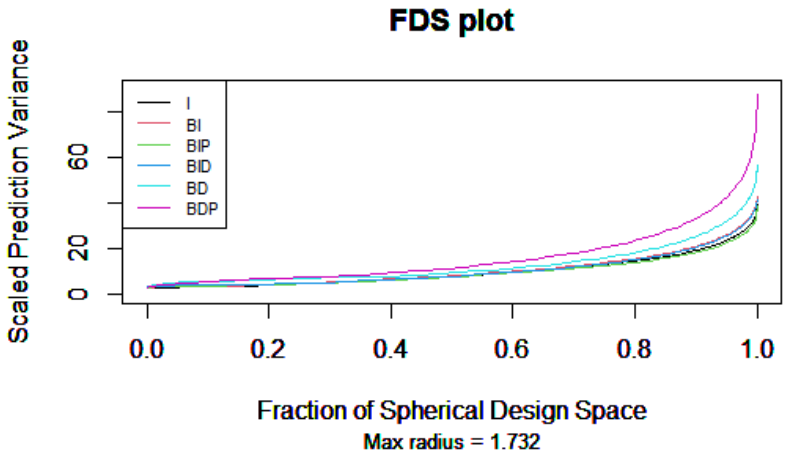

Figure 5.8: FDS Plots for 24-run I-optimal design and Bayesian optimal designs

ratio FDS plot of I-optimal design and Bayesian optimal designs. It is evident from the combined FDS plot that, the Bayesian optimal designs perform almost as good as the I-optimal design for approximatey 60% of the entire design region, where the SPV values are less than 20. For the remaining 40% of the design space where high SPV values occur, the FDS curves for Bayesian D and Bayesian DP-optimal design start deviating from the remaining designs.

However, at this point, very negligible differences are observed for Bayesian I-, Bayesian IP-, Bayesian I_D- and the I-optimal designs.

In Figure 5.9, the I-optimal design is considered as the reference de-

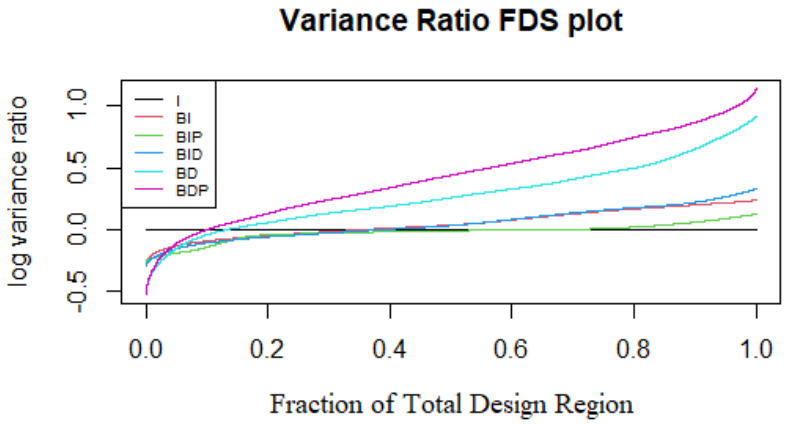

Figure 5.9: Variance Ratio FDS Plots for 24-Run I-Optimal Design and Bayesian Optimal Designs

sign. As this plot uses log variance ratio, the variation between any design and the reference design appears to be prominent. Based on all the plots, we can interpret that Bayesian IP-optimal design turn out to be slightly superior than I-optimal design, as it's curve is on the reference line of the I-optimal design or at a lower level for approximately 80% of the total design region. Bayesian I- and Bayesian I_D-optimal designs perform slightly worse than I-optimal design as their curves are above the reference line for approximately 60% of the total design space. Clearly, Bayesian D- and Bayesian DP-optimal designs are in the least preferred group when it comes to prediction ability. Therefore, we

can surmise that if the predictions are required near the origin, then all the designs can be used. If predictions are required to be made at the perimeter, then Bayesian IP-optimal design would lead to the most precise prediction among all these designs.

5.2 30-Run 4-Factor Bayesian Optimal Designs

This section contains a comparative illustrations of 30-run 4-factor Bayesian optimal designs with the 30-run 4-factor I-optimal design. Figure 5.10

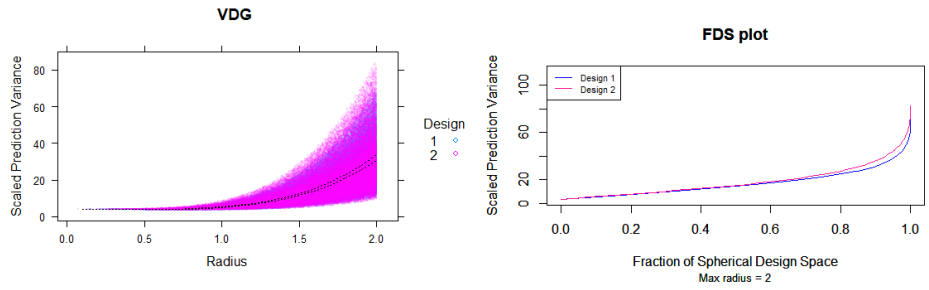

Figure 5.10: VDG and FDS plot for 30-run I-optimal design (1) and Bayesian I-optimal design (2)

shows the VDG and FDS plot for I-optimal and Bayesian I-optimal design. The VDG of the two designs reveal that the SPV distribution of both designs are mostly similar, but Bayesian I-optimal design has relatively higher average SPV values near the perimeter, possesing a higher maximum avearge SPV curve as well. FDS plot indicates that both designs have similar pattern of stable SPV values up to 70% of the whole design space. In the remaining 30% of the total design space, where SPV values are more than 25, the Bayesian

I-optimal design tends to have higher SPV values than I-optimal design.

Figure 5.11 presents the VDG and FDS plot for I- and Bayesian D-

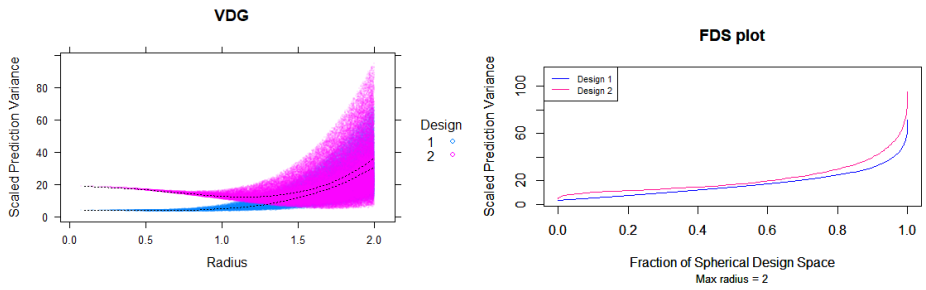

Figure 5.11: VDG and FDS plot for 30-run I-optimal design (1) and Bayesian D-optimal design (2)

optimal designs. The maximum and average SPV curves in the VDG of Bayesian D-optimal design initiate from a relatively higher position near the origin than that of I-optimal design. However, the extent of deviation between the two average SPV curves gradually tapers off near the perimeter of the design region. The FDS plot shows that the curve of Bayesian D-optimal design is consistantly at an upper level than that of the I-optimal design. Based on the figures, it is evident that Bayesian D-optimal design has higher SPV values than the I-optimal design throughout the entire design region.

Figure 5.12 displays the VDG and FDS plot for I- and Bayesian IP-optimal designs. From the VDG we can notice that even though the latter design has some higher SPV values than the former near the peripheral region, the average SPV curve of both designs are almost overlapping when the radius is less than 1.5. The FDS plot reveal that there is no significant difference in

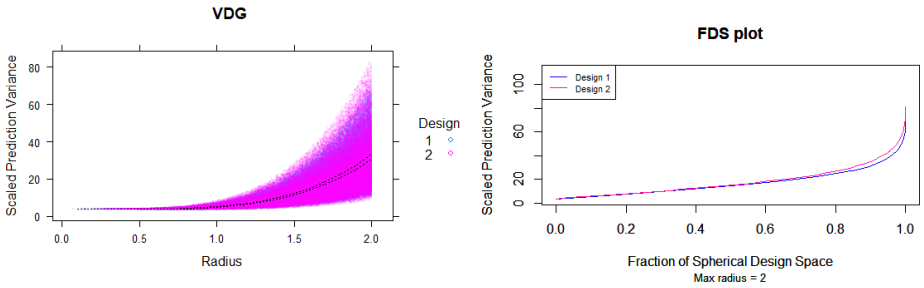

Figure 5.12: VDG and FDS plot for 30-run I-optimal design (1) and Bayesian IP-optimal design (2)

the fluctuation pattern of the SPV values of the designs for approximately 80% of the design space when SPV values for both designs are less than 37.

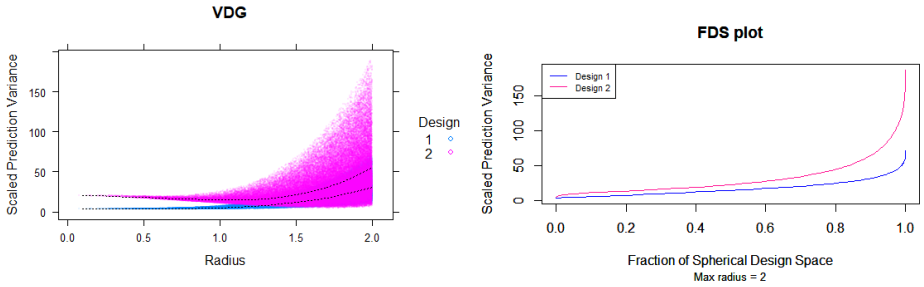

Figure 5.13: VDG and FDS plot for 30-run I-optimal design (1) and Bayesian DP-optimal design (2)

Figure 5.13 provides the VDG and FDS plot for I- and Bayesian DP-optimal designs. The VDG evidently illustrates that Bayesian DP-optimal design has a wider range of SPV values in comparison to I-optimal design. The maximum and average SPV curve of Bayesian DP-optimal design are at remarkably higher stance than that of I-optimal design thorughout the entire design region. We can observe from the FDS plot that, I-optimal design has a

relatively lower and flatter curve than Bayesian DP-optimal design, with the deviation between the two designs being noteworthy in 60% of the total design space with relatively higher SPV values.

Figure 5.14 provides the VDG and FDS plot for I- and Bayesian I_D-

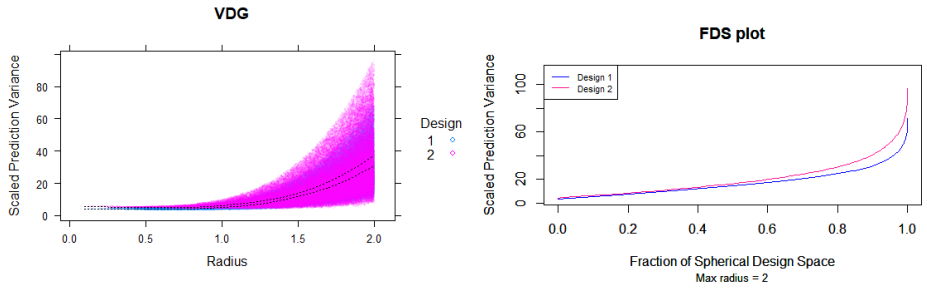

Figure 5.14: VDG and FDS plot for 30-run I-optimal design (1) and Bayesian I_D-optimal design (2)

optimal designs. We can observe from the VDG that the average SPV curve for both designs are almost similar up to radius 1.0, and Bayesian I_D-optimal design has comparatively higher SPV values after radius 1.0. The FDS plot depicts that both designs have similar pattern of fluctuation in the SPV values for approximately 60% of the design space when SPV values are around 20, after that point the difference between the two designs appears to be eminent.

Figure 5.15 presents the VDG and FDS plot for I- and Bayesian I_DP-optimal designs. The latter design seems to have relatively higher SPV values than that of the former design throughout the entire experimental region. The VDG reveal that, the difference between maximum SPV curves of the

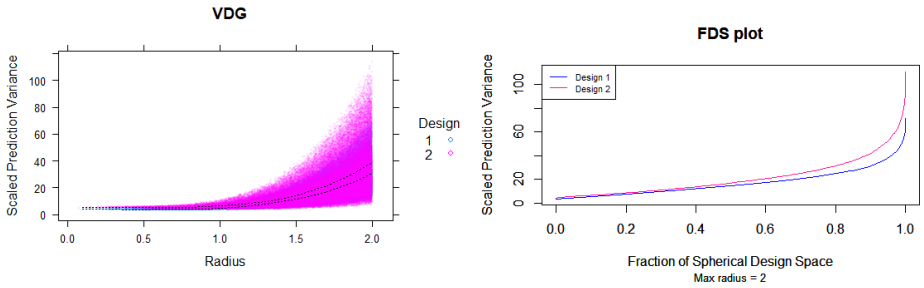

Figure 5.15: VDG and FDS plot for 30-run I-optimal design (1) and Bayesian I_DP-optimal design (2)

two designs appears prominently at the peripheral design region. The FDS plot shows that for the intial 60% of the total design space, both the designs have similar pattern of fluctuation in the SPV values, the difference becomes noteworthy in the remaining 40%, when the SPV values are greater than 20.

Figure 5.16 provides the VDG for Bayesian I, Bayesian D, Bayesian

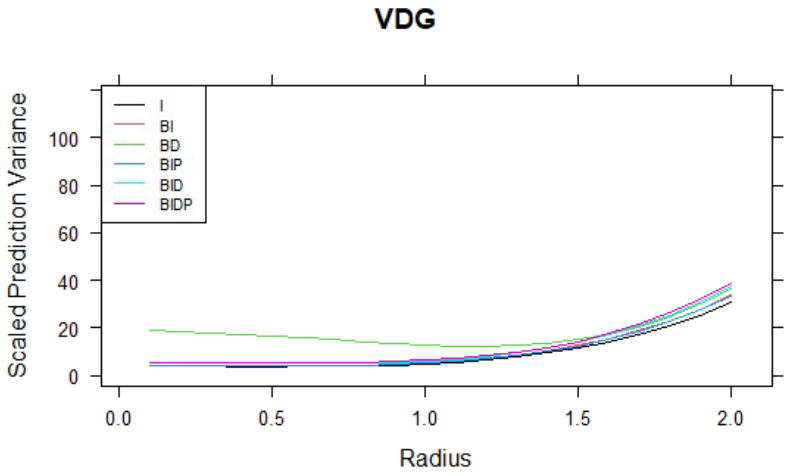

Figure 5.16: VDGs for 30-run I-optimal design and Bayesian optimal designs

IP, Bayesian I_D, Bayesian I_DP- and I-optimal designs. Each curve represents the average SPV of a design. For an enhanced illustration, Bayesian I_DP is not considered in the overall comparison, owing to it's excessively large SPV values.

Overall, from Figure 5.16 we can interpret that except for the Bayesian D-optimal design, all the other Bayesian optimal designs perform analogously with the I-optimal design. The average SPV values for Bayesian D-optimal design has comparatively higher SPV values than I-optimal design near the origin of the design region. Since, the average SPV curves for the remaining designs are close enough, for better depiction, we constructed the combined FDS plots and Variance Ratio FDS plot.

Figure 5.17 and Figure 5.18 include combined FDS plots and variance ratio FDS plot. It is evident from the combined FDS plot that, the Bayesian optimal designs perform parallelly with the I-optimal design for approximatey 60% of the entire design region, where the SPV values are around 20. In the remaining 40% of the fraction of design space where relatively higher SPV values occur, Bayesian I_DP-optimal design seems to have the FDS curve at a significantly higher level (with maximum at 111) than the other designs. On the other hand, Bayesian I and Bayesian IP-optimal designs emerge out to be almost as efficient as I-optimal design for a large fraction of the design space.

In Figure 5.18, I-optimal design is considered as the reference design.

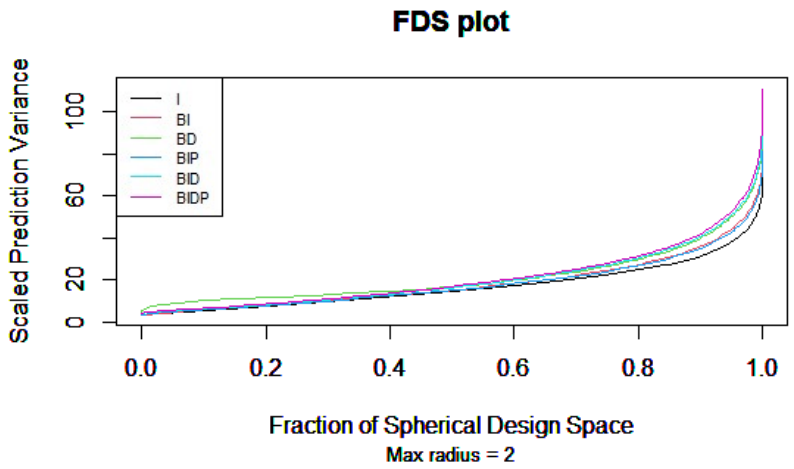

Figure 5.17: FDS plots for 30-run I-optimal design and Bayesian optimal designs

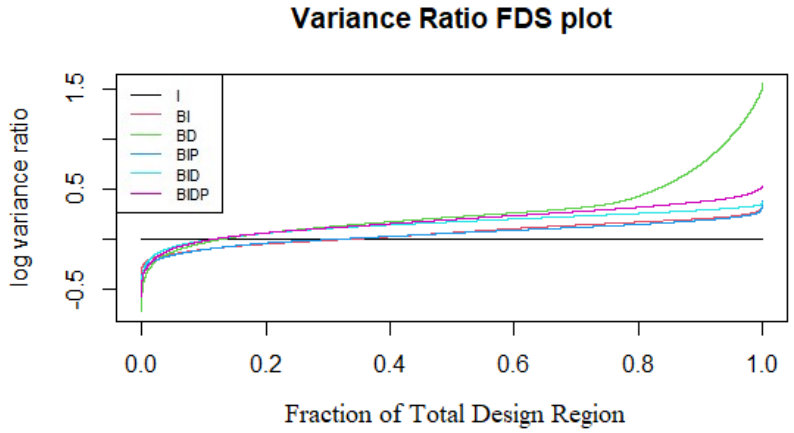

Figure 5.18: Variance Ratio FDS plots for 30-run I-optimal design and Bayesian optimal designs

From this plot, we can come to similar conclusions as the combined FDS plot, regarding the efficacy of Bayesian I- and Bayesian IP-optimal design with respect to I-optimal design. Bayesian D-optimal design is the only design having log variance ratio more than 1. Apart from Bayesian D-optimal design, the log variance ratio for all other Bayesian optimal designs are less than or equal to 0.5 for the entire design region.

Chapter 6

Conclusion and Future Work

Design of experiments is an effective implement for gaining insights on a process. These insights can help to achieve prompt refinement or augmentation. Optimal designs refers to the designs chosen from a design space, that yield the best possible outcomes in some predefined criteria. On the other hand, Bayesian optimal designs, with the same mechanism as optimal designs, facilitate accommodation of data from previous experiments and alleviate the model assumption dependency. Existing graphical techniques like VDG and FDS plot help visualize the comprehensive status of the prediction capacities of the optimal designs over the entire design region.

In this thesis, we introduced the graphical techniques to evaluate the prediction capacities of Bayesian optimal designs. These newly proposed variance dispersion graph and fraction of design space plot show the prediction propoerties of the designs and are crucial for the ultimate selection of the designs.

We evaluated the prediction capability of the 24-run 3-factor and the 30-run 4-factor Bayesian optimal designs using the graphical techniques. From our results, we learned that Bayesian I-optimal design performs notably better than Bayesian D-, Bayesian DP- and Bayesian I_DP-optimal design in terms of the magnitude and spread of SPV values. This signifies that, Bayesian I-optimal design is capable of yielding most precise prediction amongst all other Bayesian optimal designs. On the other hand, Bayesian I_D-optimal design seems to have slightly weaker performance than Bayesian I-optimal design. Surprisingly, for 24-run designs, Bayesian IP-optimal design emerged out to be better than Bayesian I-optimal design in terms of prediction abilities. So, we can deduce that, a 24-run Bayesian IP-optimal design is the ultimate choice for precise prediction in comparison to other 24-run Bayesian optimal designs, given any location of where the predictions are needed. However, for 30-run designs, the performance of these two designs was almost equivalent.

Comparing to I-optimal design, we could deduce that, for 24-run designs, Bayesian IP-optimal design turns out to be better than I-optimal design, while Bayesian I- and Bayesian I_D-optimal design function technically as well as the I-optimal design with minor deviance. However, for 30-run designs, the performance of Bayesian I- and Bayesian IP-optimal designs are similar to I-optimal design in approximately 70% the total design space. The remaining Bayesian optimal designs like Bayesian D-, Bayesian DP- and Bayesian I_DP-

optimal designs perform worse than I-optimal design for both 24- and 30-run designs throughout the entire design region.

In situations where multiple factors are involved that includes hard-to-change factors, owing to resource constraints, complete randomization of designs may not be feasible. In such situation split-plot design presents a reasonable alternative solution. It was initially used in agricultural setup where plots of land were divided into segments termed as whole plots and hard-to-change factors were assigned to each of them randomly. Each of these segments were further divided into smaller plots known as sub-plots and easy-to-change factors were applied. Construction of Bayesian split-plot optimal design has appeared in the literature. Graphical techniques for the appraisal of such Bayesian split-plot design may be developed in future, which can provide a visualization of the prediction properties of the designs over the entire experimental region.

Bibliography

Basnayake, B. M. S. C. (2019). Bayesian optimal designs with high prediction efficiency. Thesis. University of Manitoba. 3, 4, 5, 15, 17, 18, 30

Borkowski, J. J. (2003). A comparison of prediction variance criteria for response surface designs. *Journal of Quality Technology 35*(1), 70–77. 35

Box, G. E. P. and J. S. Hunter (1957). Multi-factor experimental designs for exploring response surfaces. *The Annals of Mathematical Statistics 28*(1), 195–241. 24

Chaloner, K. and I. Verdinelli (1995). Bayesian experimental design: a review. *Statistical Science 10*(3), 273–304. 3

de Oliveira, H. M., C. B. A. de Oliveira, S. G. Gilmour, and L. A. Trinca (2019). Prediction properties of optimum response surface designs. arXiv.1906.07500. 3, 12, 13, 17

DuMouchel, W. and B. A. Jones (1994). A simple bayesian modification of

d-optimal designs to reduce dependence on an assumed model. *Technometrics 36*, 37–47. 3, 14

Gilmour, S. G. and L. A. Trinca (2012). Optimum design of experiments for statistical inference. *Applied Statistics 61*(3), 345–401. 3, 8, 12, 16, 17

Giovannitti-Jensen, A. and R. H. Myers (1989). Graphical assessment of the prediction capability of response surface designs. *Technometrics 31*(2), 159–171. 4, 18, 22

Goldfarb, H. B., C. M. Anderson-Cook, C. M. Borror, and D. C. Montgomery (2004). Fraction of design space plots for assessing mixture and mixture-process designs. *Journal of Quality Technology 36*(2), 169–179. 35

Hussey, J. R., R. H. Myers, and E. C. Houck (1987). Correlated simulation experiments in first-order response surface design. *Operations Research 35*(5), 744–758. 21

Jones, B. and P. Goos (2012). I-optimal versus d-optimal split-plot response surface designs. *Journal of Quality Technology 44*(2), 85–101. 2, 9

Khuri, A. I., H.-J. Kim, and Y. Um (1996). Quantile plots of the prediction variance for response surface designs. *Computational Statistics & Data Analysis 22*, 395–407. 23

Kiefer, J. and J. Wolfowitz (1959). Optimum designs in regression problems. *The Annals of Mathematical Statistics 30*(2), 271–294. 1

Leonard, R. D. and D. J. Edwards (2017). Bayesian D-optimal screening experiments with partial replication. *Computational Statistics and Data Analysis 115*, 79–90. 3, 16

Lindley, D. V. (1972). *Bayesian Statistics, A Review*. Society for Industrial and Applied Mathematics. 14

Lupinacci, P. J. and J. G. Pigeon (2008). A class of partially replicated two-level fractional factorial designs. *Journal of Quality Technology 40*(2), 184–193. 2

Ozol-Godfrey, A. (2004). *Understanding scaled prediction variance using graphical methods for model robustness, measurement error and generalized linear models for response surface designs. Thesis.* Virginia Polytechnic Institute and State University. 35, 36

Schoonees, P., N. Le Roux, and R. Coetzer (2016). Flexible graphical assessment of experimental designs in r: the vdg package. *Journal of Statistical Software 74*, 1–22. 22, 34, 36

Smith, K. (1918). On the standard deviations of adjusted and interpolated values of an observed polynomial function and its constants and the guidance they give towards a proper choice of the distribution of observations. *Biometrika 12*, 1–85. 1

Trinca, L. A. and S. G. Gilmour (1999). Difference variance dispersion graphs

for comparing response surface designs with applications in food technology. *Applied Statistics 48*(4), 441–455. 2, 12

Tsai, S.-F. and C.-T. Liao (2014). Selection of partial replication on two-level orthogonal arrays. *Canadian Journal of Statistics 42*(1), 168–183. 2

Wald, A. (1943). On the efficient design of statistical investigations. *The Annals of Mathematical Statistics 14*(2), 134–140. 2, 7

Zahran, A., C. M. Anderson-Cook, and R. H. Myers (2003). Fraction of design space to assess prediction capability of response surface designs. *Journal of Quality Technology 35*(4), 377–386. 4, 26, 35

Appendix A

Appendix

Table A.1: 24-run three-level Bayesian I-, Bayesian D- and Bayesian DP-Optimal Designs with 3 factors.

Run	Bayesian I			Bayesian D			Bayesian DP		
	X1	X2	X3	X1	X2	X3	X1	X2	X3
1	1	-1	1	-1	1	1	1	-1	1
2	1	-1	-1	1	-1	1	-1	1	-1
3	0	0	-1	-1	1	1	-1	1	1
4	0	0	0	-1	0	0	0	1	0
5	0	0	0	-1	-1	1	-1	1	1
6	1	1	1	-1	-1	1	0	1	0
7	0	0	0	-1	-1	-1	0	0	1
8	0	1	-1	1	-1	1	1	-1	-1
9	-1	0	1	1	0	0	1	-1	1
10	1	1	0	1	-1	-1	0	0	1
11	-1	0	-1	1	1	-1	-1	0	0
12	0	-1	0	-1	1	-1	-1	-1	-1
13	1	0	1	-1	1	-1	1	1	1
14	0	-1	1	1	1	1	1	1	-1
15	-1	1	1	1	1	0	1	-1	-1
16	0	0	0	0	0	-1	0	0	1
17	-1	-1	1	0	0	1	-1	-1	-1
18	-1	1	-1	1	0	-1	-1	0	0
19	-1	1	0	1	1	1	1	1	1
20	1	0	0	0	-1	0	1	1	-1
21	-1	-1	0	0	1	-1	-1	-1	1
22	0	1	1	-1	-1	-1	-1	0	0
23	1	1	-1	1	-1	-1	-1	-1	1
24	-1	-1	-1	0	1	0	-1	1	-1

Table A.2: 24-run three-level Bayesian IP-, Bayesian I_D- and Bayesian I_DP-Optimal Designs with 3 factors.

Run	Bayesian IP			Bayesian I_D			Bayesian I_DP		
	X1	X2	X3	X1	X2	X3	X1	X2	X3
1	0	-1	0	1	1	1	1	-1	1
2	1	0	0	-1	-1	1	1	1	1
3	0	-1	0	0	0	0	1	-1	-1
4	1	0	0	0	0	0	-1	1	-1
5	0	0	1	1	1	-1	1	-1	-1
6	1	-1	-1	0	0	0	-1	-1	-1
7	0	-1	0	1	-1	-1	-1	-1	-1
8	0	0	-1	0	1	1	-1	1	1
9	-1	-1	-1	0	0	0	-1	1	1
10	0	0	1	1	-1	1	0	0	-1
11	-1	0	0	-1	0	1	1	0	0
12	0	0	-1	-1	0	-1	0	1	0
13	-1	-1	1	1	1	0	-1	-1	1
14	-1	0	0	1	-1	0	1	0	0
15	0	1	0	-1	1	-1	1	-1	1
16	1	-1	1	-1	-1	-1	1	1	1
17	0	1	0	0	-1	1	1	1	-1
18	0	0	-1	-1	1	0	0	0	-1
19	-1	0	0	1	0	1	0	1	0
20	-1	1	1	-1	-1	0	-1	0	0
21	-1	1	-1	1	0	-1	-1	1	-1
22	1	1	-1	0	1	-1	0	0	1
23	0	1	0	-1	1	1	1	1	-1
24	1	1	1	0	-1	-1	0	-1	0

Table A.3: 30-run three-level I-, Bayesian I- and Bayesian D-Optimal Designs with 4 factors.

Run	I				Bayesian I				Bayesian D			
	X1	X2	X3	X4	X1	X2	X3	X4	X1	X2	X3	X4
1	0	0	1	-1	0	0	0	1	1	1	-1	1
2	0	0	0	0	1	1	-1	-1	-1	-1	-1	1
3	0	0	-1	0	0	0	0	0	-1	1	1	1
4	-1	-1	0	-1	1	-1	0	-1	1	-1	1	1
5	0	-1	0	0	0	0	0	0	1	1	-1	-1
6	0	0	0	0	0	-1	1	1	1	-1	-1	1
7	0	1	-1	1	1	1	1	0	1	-1	-1	-1
8	1	1	0	-1	1	0	-1	0	1	1	1	1
9	0	0	0	0	1	1	0	1	-1	1	-1	1
10	-1	1	1	-1	1	0	1	1	1	-1	1	0
11	-1	0	1	0	0	-1	-1	-1	-1	-1	1	1
12	-1	0	0	1	0	1	-1	1	1	1	1	-1
13	-1	-1	0	1	-1	1	1	1	0	1	-1	-1
14	1	0	-1	1	-1	1	-1	0	-1	-1	1	-1
15	0	-1	1	1	-1	0	-1	1	-1	1	1	-1
16	-1	-1	-1	0	0	0	0	0	-1	0	-1	-1
17	-1	1	-1	0	1	-1	-1	1	0	0	0	1
18	1	-1	-1	-1	0	0	0	0	1	-1	0	-1
19	0	1	0	0	-1	-1	1	-1	0	-1	-1	0
20	1	1	1	1	-1	1	0	-1	0	-1	1	-1
21	0	-1	0	-1	0	0	0	0	-1	-1	-1	-1
22	1	0	-1	-1	0	1	0	0	-1	1	-1	0
23	0	1	-1	-1	1	0	1	-1	1	0	-1	1
24	1	1	0	0	-1	0	1	0	-1	1	0	-1
25	0	0	0	0	-1	0	-1	-1	-1	-1	0	1
26	1	0	0	0	-1	-1	-1	0	-1	0	1	0
27	1	-1	1	0	0	0	0	0	1	-1	1	1
28	0	0	0	1	0	1	1	-1	1	0	1	-1
29	0	0	1	0	1	-1	1	0	0	1	1	1
30	-1	0	0	-1	-1	-1	0	1	1	1	0	0

Table A.4: 30-run three-level Bayesian IP- and Bayesian DP-Optimal Designs with 4 factors.

Run	Bayesian IP				Bayesian DP			
	X1	X2	X3	X4	X1	X2	X3	X3
1	0	1	0	0	1	-1	-1	-1
2	-1	0	1	1	-1	1	-1	-1
3	1	0	0	0	1	-1	-1	1
4	-1	0	0	0	1	-1	-1	-1
5	-1	1	1	-1	-1	1	-1	1
6	0	0	0	-1	-1	-1	1	1
7	0	0	0	-1	-1	-1	1	-1
8	-1	-1	-1	0	-1	-1	1	-1
9	0	0	0	-1	-1	1	1	0
10	-1	1	-1	-1	1	1	1	-1
11	-1	-1	-1	0	1	1	1	-1
12	0	-1	0	1	1	-1	-1	1
13	1	1	-1	-1	1	1	0	1
14	0	1	0	0	-1	-1	-1	0
15	1	0	-1	1	1	1	0	1
16	0	0	-1	0	1	0	1	1
17	1	1	1	-1	-1	1	-1	-1
18	0	-1	0	1	1	0	1	1
19	0	0	1	0	-1	-1	1	1
20	0	0	1	0	1	-1	1	0
21	1	-1	-1	-1	1	1	-1	0
22	0	0	-1	0	1	1	-1	0
23	-1	-1	1	-1	1	-1	1	0
24	-1	0	0	0	-1	1	1	0
25	1	-1	1	0	0	1	1	1
26	1	1	1	1	-1	-1	-1	0
27	0	1	0	0	0	0	0	-1
28	1	0	0	0	0	1	1	1
29	1	-1	1	0	0	0	0	-1
30	-1	1	-1	1	-1	1	-1	1

Table A.5: 30-run three-level Bayesian I_D- and Bayesian I_DP-Optimal Designs with 4 factors.

Run	Bayesian I_D				Bayesian I_DP			
	X1	X2	X3	X4	X1	X2	X3	X4
1	-1	1	1	1	0	0	0	0
2	-1	1	-1	-1	0	0	0	0
3	0	-1	0	0	1	-1	1	0
4	-1	1	-1	1	1	1	1	-1
5	-1	1	1	-1	-1	-1	0	-1
6	-1	-1	-1	-1	1	0	-1	-1
7	1	-1	1	1	-1	1	-1	-1
8	1	1	1	1	0	0	0	0
9	-1	-1	-1	1	0	-1	-1	1
10	1	1	-1	-1	-1	1	1	0
11	1	1	-1	1	0	0	0	0
12	1	-1	1	-1	1	1	-1	1
13	1	-1	-1	1	-1	1	-1	-1
14	-1	-1	1	1	-1	-1	1	1
15	-1	0	0	-1	-1	-1	-1	0
16	0	0	1	0	1	0	1	1
17	1	1	1	-1	1	0	1	1
18	1	0	0	0	0	1	1	1
19	0	0	0	1	0	0	0	0
20	-1	-1	1	-1	-1	-1	0	-1
21	0	-1	0	0	1	-1	0	1
22	1	-1	-1	-1	-1	0	-1	1
23	-1	0	-1	0	-1	0	-1	1
24	0	1	-1	0	1	1	-1	1
25	-1	1	0	0	-1	1	0	1
26	0	0	0	1	1	1	1	-1
27	0	0	1	0	1	-1	-1	-1
28	1	0	0	0	0	-1	1	-1
29	0	0	-1	-1	0	-1	1	-1
30	0	1	0	-1	-1	0	1	-1